

Theory for the optimal detection of time-varying signals in cellular sensing systems

G. Malaguti¹ and P.R. ten Wolde¹

¹*AMOLF, Science Park 104, 1098 XG Amsterdam, The Netherlands*

(Dated: August 20, 2021)

Living cells often need to measure chemical concentrations that vary in time. To this end, they deploy many resources such as receptors, downstream signaling molecules, time and energy. Here, we present a theory for the optimal design of a large class of sensing systems that need to detect time-varying signals, a receptor driving a push-pull network. The theory is based on the concept of the dynamic input-output relation, which describes the mapping between the current ligand concentration and the average receptor occupancy over the past integration time. This concept is used to develop the idea that the cell employs its push-pull network to estimate the receptor occupancy and then uses this estimate to infer the current ligand concentration by inverting the dynamic input-output relation. The theory reveals that the sensing error can be decomposed into two terms: the sampling error in the estimate of the receptor occupancy and the dynamical error that arises because the average ligand concentration over the past integration time may not reflect the current ligand concentration. The theory generalizes the design principle of optimal resource allocation previously identified for static signals, which states that in an optimally designed sensing system the three fundamental resource classes of receptors and their integration time, readout molecules, and energy are equally limiting so that no resource is wasted. However, in contrast to static signals, receptors and power cannot be traded freely against time to reach a desired sensing precision: there exists an optimal integration time that maximizes the sensing precision, which depends on the number of receptors, the receptor correlation time, and the correlation time and variance of the input signal. Applying our theory to the chemotaxis system of *Escherichia coli* indicates that this bacterium has evolved to optimally sense shallow gradients.

PACS numbers: 87.10.Vg, 87.16.Xa, 87.18.Tt

I. INTRODUCTION

Living cells often need to sense and respond to chemical signals that vary in time. This is particularly true for cells that navigate through their environment. Interestingly, experiments have revealed that cells can measure chemical concentrations with high precision [1–3]. This raises the question how accurately cells can measure time-varying signals.

Cells measure chemical concentrations via receptors on their surface. These measurements are inevitably corrupted by the stochastic arrival of the ligand molecules by diffusion and by the stochastic binding of the ligand to the receptor. Berg and Purcell pointed out that cells can increase the number of measurements to reduce the sensing error in two principal ways [1]. One is to simply increase the number of receptors. The other is to take more measurements per receptor; here, the cell infers the concentration not from the instantaneous number of ligand-bound receptors, but rather from the average receptor occupancy over an integration time [1]. While many studies have addressed the question how time integration sets the fundamental limit to the precision of sensing static concentrations [4–16] (for review, see [17]), how accurately time integration can be performed for time-varying signals is a wide-open question [18]. A theory that can describe how the sensing precision depends on the design of the system and predict what the optimal design is that maximizes the sensing precision is lacking.

Biochemical networks that implement the mechanism

of time integration require cellular resources to be built and run. Receptors and time are needed to take the concentration measurements, downstream molecules are necessary to store the ligand-binding states of the receptor in the past, and energy is required to store these states reliably. In a previous study on sensing static signals that do not vary on the timescale of the cellular response, we showed that three resource classes—receptors and their integration time, readout molecules, and energy—fundamentally limit sensing like weak links in a chain [12]. This yields the design principle of optimal resource allocation, which states that in an optimally designed system each resource class is equally limiting so that no resource is in excess [12]. Within these classes, resources can be traded freely against each other: time can not only be traded against receptors—a system consisting of one receptor that takes many measurements over time can reach the same sensing precision as one containing many receptors that take one measurement each—but also against power—many noisy measurements can provide the same information as one reliable measurement.

Cells live, however, in a highly dynamic environment and they often respond on a timescale that is comparable to that on which the input signal varies. Examples are cells (or nuclei) that during embryonic development differentiate in response to time-varying morphogen gradients [19] or cells that navigate through their environment [20–22]; these cells shape, via their movement, the statistics of the input signal, creating a correlation time of the input signal that is comparable to the timescale of the response. In these scenarios, the accuracy of sens-

ing depends not only on properties of the cellular sensing system, but also on the dynamics of the input signal. It is indeed far from clear whether the design principles uncovered for systems sensing static concentrations [12] also hold for those that need to detect time-varying signals. In particular, for sensing time-varying signals we expect that time itself becomes a fundamental resource. A longer integration time will not only reduce the receptor noise but also distort the input signal [18, 23]. This raises many questions: Can the design principle of optimal resource allocation be generalized to time-varying signals? If so, what does it predict for the optimal design of the system? How does that depend on the statistics of the input signal? In particular, how does the power and the number of receptor and readout molecules required to maintain a desired sensing precision depend on the timescale and the strength of the input fluctuations?

To address these questions we present a theory for the optimal design of cellular sensing systems that need to measure time-varying ligand concentrations. The theory applies to the large class of systems in which a receptor drives a push-pull network [24]. These systems are omnipresent in prokaryotic and eukaryotic cells [25]. Examples are GTPase cycles, as in the Ras system, phosphorylation cycles, as in MAPK cascades, and two-component systems like the chemotaxis system of *Escherichia coli*. These systems employ the mechanism of time integration, in which the ligand concentration is inferred from the average receptor occupancy over the past integration time [12]. We thus do not consider the sensing strategy of maximum-likelihood estimation, in which the concentration is estimated from the duration of the unbound receptor state [7, 9, 17, 26, 27].

To develop a unified theory of sensing, we combine ideas on information transmission via time-varying signals from Refs. [28–30] with the sampling framework from Ref. [12]. Our theory is based on a new concept, the *dynamic* input-output relation $p_{\tau_r}(L)$, which describes the mapping between the average receptor occupancy p_{τ_r} over the past integration time τ_r and the current concentration L ; it differs fundamentally from the conventional static input-output relation, because it takes into account the dynamics of the input signal and the finite response time of the system. The dynamic input-output relation allows us to develop the notion that the cell employs its push-pull network to estimate the receptor occupancy and then uses this estimate to infer the current concentration, by inverting $p_{\tau_r}(L)$. Our theory reveals that the sensing error can be decomposed into two terms, which each have a clear intuitive interpretation. One term, the sampling error, describes the sensing error that arises from the finite accuracy by which the receptor occupancy is estimated. This error depends on the number of receptor samples as set by the number of readout molecules and the integration time; their independence as given by the receptor-sampling interval and the receptor-ligand correlation time; and their reliability as determined by fuel turnover. The other term is the

dynamical error, and is related to the error introduced in [30]. This error is determined by how much the concentration in the past integration time reflects the current concentration that the cell aims to estimate; it depends besides the integration time on the timescale on which the input varies.

Our theory gives a comprehensive view on the optimal design of a cellular sensing system. Firstly, it reveals that the resource allocation principle of [12] can be generalized to time-varying signals. There exist three fundamental resource classes—receptors and their integration time, readout molecules, and power and integration time—which each fundamentally limit the accuracy of sensing; and, in an optimally designed system, each resource class is equally limiting the sensing precision. The optimal resource allocation principle thus gives the relationship between receptors, integration time, readout molecules, and power so that none of these cellular resources is in excess and thus wasted. However, in contrast to sensing static signals, time cannot be freely traded against the number of receptors and the power to achieve a desired sensing precision: there exists an optimal integration time that maximizes the sensing precision, which arises as a trade-off between the sampling error and the dynamical error. This optimal integration time depends on the statistics of the input signal and on the number of receptors. Together with the resource allocation principle it completely specifies the optimal design of the system in terms of its resources protein copies, time, and energy.

Our theory also makes a number of specific predictions. The optimal integration time decreases as the number of receptors is increased, because this allows for more instantaneous measurements. It also decreases when the input signal varies more rapidly and/or more strongly. Moreover, our allocation principle reveals that when the input signal varies more rapidly, both the number of receptors and the power must increase to maintain a desired sensing precision, while the number of readout molecules does not. Finally, we test our prediction for the optimal integration time for the chemotaxis system of *Escherichia coli*; this analysis indicates that the chemotaxis system has evolved to optimally sense shallow concentration gradients.

II. THEORY

A. The set up of the problem

We consider a single cell that needs to sense a time-varying ligand concentration $L(t)$, see Fig. 1(a). The ligand concentration dynamics is modeled as a stationary Markovian signal specified by the mean (total) ligand concentration \bar{L} , the variance σ_L^2 and the correlation time $\tau_L = \lambda^{-1}$, which sets the timescale of the input fluctuations. It obeys Gaussian statistics [28].

The concentration is measured via R_T receptor pro-

teins on the cell surface, which independently bind the ligand [17], $L + R \xrightleftharpoons[k_2]{k_1} RL$. The correlation time of the receptor state is given by $\tau_c = 1/(k_1\bar{L} + k_2)$. It determines the timescale on which independent concentration measurements can be made. Denoting the average number of ligand-bound receptors as \overline{RL} , the receptor occupancy is $p = \overline{RL}/R_T = k_1\bar{L}\tau_c$. This shows that for a given p the correlation time $\tau_c = p/(k_1\bar{L}) = \mu^{-1}$ is fundamentally bounded by the ligand concentration \bar{L} and the ligand diffusion constant, which limits the binding rate k_1 [1, 4, 14, 17].

The ligand-binding state of the receptor is read out via a push-pull network [24], which is a common non-equilibrium signaling motif in prokaryotic and eukaryotic cells [25]. In this system, fuel turnover is used to drive the chemical modification of a downstream readout protein x , see Fig. 1(b). The most common scheme is phosphorylation fueled by the hydrolysis of adenosine triphosphate (ATP). The receptor, or an enzyme associated with it such as CheA in *E. coli*, catalyzes the modification of the readout, $x + RL + ATP \rightleftharpoons x^* + RL + ADP$. The active readout proteins x^* can decay spontaneously or be deactivated by an enzyme, such as CheZ in *E. coli*, $x^* \rightleftharpoons x + Pi$. Inside the living cell the system is maintained in a non-equilibrium steady state by keeping the concentrations of ATP, ADP (adenosine diphosphate) and Pi (inorganic phosphate) constant. We absorb their concentrations and the activities of the kinase and, if applicable, phosphatase in the (de)phosphorylation rates, coarse-graining the modification into instantaneous second order reactions: $x + RL \xrightleftharpoons[k_{-f}]{k_f} x^* + RL$, $x^* \xrightleftharpoons[k_{-r}]{k_r} x + Pi$.

This system has a relaxation time $\tau_r = 1/[(k_f + k_{-f})\overline{RL} + k_r + k_{-r}] = \mu'^{-1}$. It sets the lifetime of the active readout molecules, which determines how long these molecules can carry information on the ligand binding state of the receptor. The relaxation time τ_r thus sets the integration time of the receptor state.

The deviations of RL and x^* away from their steady-state values are given by (see section S-I of the SI):

$$\delta\dot{RL}(t) = \rho\delta L(t) - \mu\delta RL(t) + \eta_{RL}, \quad (1)$$

$$\delta\dot{x}^*(t) = \rho'\delta RL(t) - \mu'\delta x^*(t) + \eta_{x^*}, \quad (2)$$

where ρ and ρ' are functions of the rate constants and the noise terms η_{RL}, η_{x^*} model the noise in receptor-ligand binding and readout phosphorylation, respectively.

B. The cell sensing precision

Signal-to-noise ratio

The time-varying ligand concentration has a distribution of instantaneous values $L(t)$, and we would like to know how many of these the system can resolve. To this end

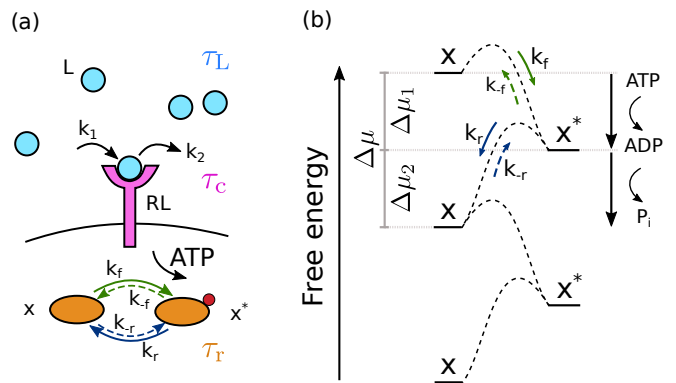


FIG. 1. The cell signaling network. (a) The time-varying ligand concentration is modeled as a Markovian signal with mean \bar{L} , variance σ_L^2 and correlation time $\tau_L = \lambda^{-1}$. A free ligand molecule L (light blue circle) can bind at rate k_1 to a free receptor R (magenta protein) on the cell membrane (black line), forming the complex RL , and unbind at rate k_2 from RL . The correlation time of the receptor state is τ_c . The complex RL catalyzes the phosphorylation reaction, driven by ATP conversion, of a downstream readout from the unphosphorylated (inactive) state x to the phosphorylated (active) state x^* , with rate k_f . The phosphorylated readout then spontaneously decays to the x state with rate k_r . Microscopic reverse reactions of each signaling pathway are represented by dashed arrows. The relaxation time of the push-pull network is τ_r . (b) Free-energy landscape of a readout molecule across the activation/deactivation reactions. Fuel turnover, provided by ATP conversion, drives the activation (phosphorylation) reaction characterized by the forward rate k_f and its microscopic reverse rate k_{-f} (green arrows). Associated with this activation reaction is a free-energy drop $\Delta\mu_1 = \log \frac{k_f \bar{x}}{k_{-f} \bar{x}^*}$. The deactivation pathway corresponds to the spontaneous release of the inorganic phosphate; it is characterized by the rate k_r and its microscopic reverse k_{-r} (blue arrows) and corresponds to a free-energy drop $\Delta\mu_2 = \log \frac{k_r \bar{x}^*}{k_{-r} \bar{x}}$.

we define the signal-to-noise ratio (SNR), see Fig. 2(a):

$$\text{SNR} := \frac{\sigma_L^2}{(\delta\hat{L})^2}. \quad (3)$$

Here σ_L^2 is the variance of the ligand concentration $L(t)$; it is a measure for the total number of input states. The quantity $(\delta\hat{L})^2$ is the error in the estimate of the current ligand concentration. The signal-to-noise ratio thus quantifies the number of distinct ligand concentrations that the system can resolve. Since the system is stationary and time invariant, we can omit the argument in $L(t)$ and write $L = L(t)$.

Inferring concentration from readout

The cell estimates the current ligand concentration $L(t)$ from the instantaneous number of active readout molecules $x^*(t)$. In the Gaussian model employed here, we can calculate the SNR defined by Eq. 3, and it is related to the mutual information $I(x^*; L) = 1/2 \ln(1 + \text{SNR})$ between the input L and the output x^* (section

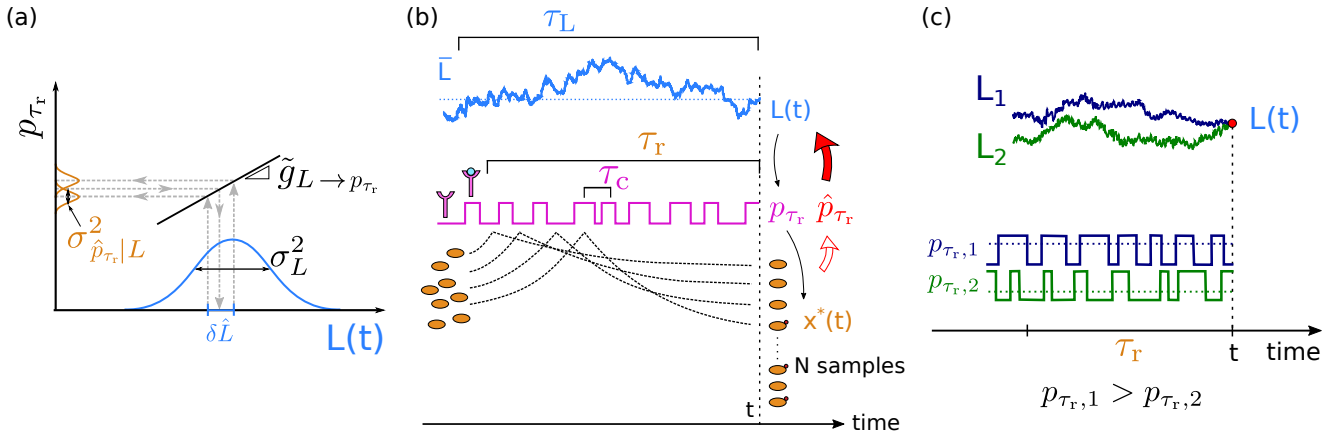


FIG. 2. **The precision of estimating a time-varying ligand concentration $L(t)$.** (a) The cell estimates the current ligand concentration $L(t)$ by estimating the average receptor occupancy p_{τ_r} over the past integration time τ_r and by inverting the dynamic input-output relation $p_{\tau_r}(L)$. The error in the estimate of the concentration $(\delta \hat{L})^2 = \sigma_{\hat{p}_{\tau_r}|L}^2 / \tilde{g}_{L \rightarrow p_{\tau_r}}^2$ depends on the variance $\sigma_{\hat{p}_{\tau_r}|L}^2$ in the estimate of the average receptor occupancy \hat{p}_{τ_r} , and the dynamic gain $\tilde{g}_{L \rightarrow p_{\tau_r}}$, the slope of $p_{\tau_r}(L)$, which determines how the error in \hat{p}_{τ_r} propagates to that in $\delta \hat{L}$. The input distribution has width σ_L^2 . (b) The average receptor occupancy p_{τ_r} over the past integration time τ_r is estimated via the downstream network, which is modelled as a device that discretely samples the ligand-binding state of the receptor via its readout molecules x [12]; the fraction of modified readout molecules provides an estimate of p_{τ_r} , see Eq. 7. The sensing error has two contributions, Eq. 20: the sampling error and the dynamical error. The sampling error arises from the error in the estimate of p_{τ_r} that is due to the stochasticity of the sampling process; it depends on the number of samples, their independence and their accuracy. (c) The dynamical error arises because the current ligand concentration $L(t)$ is estimated via the average receptor occupancy p_{τ_r} over the past integration time τ_r : the latter depends on the ligand concentration in the past τ_r , which will, in general, deviate from the current concentration. Two different input trajectories (L_1 in blue, L_2 in green) ending at time t at the *same* value $L(t)$ (red dot) lead to different estimates of $L(t)$, due to their different average receptor occupancy ($p_{\tau_r,1} > p_{\tau_r,2}$) in the past τ_r .

S-II SI). However, the resulting expression for the SNR is not very instructive (Eq. S21):

$$\begin{aligned} \text{SNR}^{-1} &= \frac{(\lambda + \mu)^2 (\lambda + \mu')^2}{\rho^2 \rho'^2 \sigma_L^2} f(1-f) X_T \\ &+ \frac{(\lambda + \mu)^2 (\lambda + \mu')^2}{\sigma_L^2 \mu' (\mu + \mu') \rho^2} p(1-p) R_T \\ &+ \frac{(\lambda + \mu)(\lambda + \mu')(\lambda + \mu + \mu')}{\mu \mu' (\mu + \mu')} - 1. \end{aligned} \quad (4)$$

This approach cannot elucidate the design logic of the system, because it treats the signal transmission from the input L to the output x^* as a black box. The central quantity in this calculation is the covariance σ_{L,x^*}^2 between the ligand $L(t)$ and the readout $x^*(t)$ (see section S-II), which does not reveal how the signal is relayed from the input to the output. To elucidate the system's design principles, we have to open the black box: we need to recognize that the input signal is transmitted to the output via the receptor, and that the cell does not estimate the ligand concentration from x^* directly, but rather via its receptor (see Fig. 1). We can indeed arrive at a much more illuminating form of the same result as Eq. 4 by starting from the notion that the cell uses its readout system to estimate the receptor occupancy, from which the ligand concentration is then inferred. However, to develop this notion into a theory,

we need new concepts, which we describe next.

Inferring concentration from receptor occupancy

The central idea of our theory is illustrated in Fig. 2a: the cell employs the push-pull network to estimate the average receptor occupancy p_{τ_r} over the past integration time τ_r , and then uses this estimate $\hat{p}_{\tau_r}|L$ to infer the current concentration L by inverting the mapping $p_{\tau_r}(L)$. The sensing error is then determined by how accurately the cell estimates p_{τ_r} and how the error in $\hat{p}_{\tau_r}|L$ propagates to that in L , which is determined by $p_{\tau_r}(L)$. We now first give an overview of the central concepts.

Dynamic input-output relation The mapping $p_{\tau_r}(L)$ is the *dynamic input-output relation*. It gives the average receptor occupancy over the past integration time τ_r *given* that the *current* value of the input signal is $L = L(t)$, see Fig. 2(a). Here, the average is not only over the noise in receptor-ligand binding and readout activation (Fig. 2(b)), but also over the subensemble of past input trajectories that each end at the same current concentration L (Fig. 2(c)) [28–30]. In contrast to the conventional, static input-output relation $p(L_s)$, which gives the average receptor occupancy p for a steady-state ligand concentration L_s that does not vary in time, the dynamic input-output relation takes into account the dynamics of the input signal and the finite response time of the system. It depends on all the timescales in the problem: the timescale of the input, τ_L , the receptor-

ligand correlation time τ_c , and the integration time τ_r . Only when $\tau_L \gg \tau_c, \tau_r$, does the dynamic input-output relation $p_{\tau_r}(L)$ become equal to the static input-output relation $p(L_s)$.

Sensing error Linearizing the dynamic input-output relation $p_{\tau_r}(L)$ around the mean ligand concentration \bar{L} (see Fig. 2a) and using the rules of error propagation, the expected error in the concentration estimate is then

$$(\delta\hat{L})^2 = \frac{\sigma_{\hat{p}_{\tau_r|L}}^2}{\tilde{g}_{L \rightarrow p_{\tau_r}}^2}. \quad (5)$$

Here $\sigma_{\hat{p}_{\tau_r|L}}^2$ is the variance in the estimate $\hat{p}_{\tau_r|L}$ of the average receptor occupancy over the past τ_r given that the current input signal is L , see Fig. 2(a). The quantity $\tilde{g}_{L \rightarrow p_{\tau_r}}$ is the *dynamic gain*, which is the slope of the dynamic input-output relation $p_{\tau_r}(L)$; it determines how much an error in the estimate of p_{τ_r} propagates to that in L . Eq. 5 generalizes the expression for the error in sensing static concentrations [1, 4, 5, 10, 12, 14, 17] to that of time-varying concentrations.

SNR Combining Eqs. 5 and 3 yields the signal-to-noise ratio:

$$\text{SNR} = \frac{\tilde{g}_{L \rightarrow p_{\tau_r}}^2}{\sigma_{\hat{p}_{\tau_r|L}}^2} \sigma_L^2. \quad (6)$$

Estimating the receptor occupancy To derive the error in estimating p_{τ_r} , $\sigma_{\hat{p}_{\tau_r|L}}^2$, we view, following our earlier work [12], the push-pull network as a device that discretely samples the receptor state (see Fig. 2(b)). The principle is that cells employ the activation reaction $x + RL \rightarrow x^* + RL$ to store the state of the receptor in stable chemical modification states of the readout molecules. Readout molecules that collide with a ligand-bound receptor are modified, while those that collide with an unbound receptor are not (Fig. 2(b)). The readout molecules serve as samples of the receptor at the time they were created, and collectively they encode the history of the receptor. The average receptor occupancy p_{τ_r} over the past integration time τ_r is thus estimated from the current number of active readout molecules $x^*(L(t)) = x^*(L)$:

$$\hat{p}_{\tau_r|L} = \frac{x^*(L)}{\bar{N}}, \quad (7)$$

where \bar{N} is the average number of samples obtained during τ_r . To determine the effective number of independent samples, we need to consider not only the creation of the samples, but also their decay and accuracy. Samples decay via the deactivation reaction $x^* \rightarrow x$, which means that they only provide information on the receptor occupancy over the past τ_r . In addition, both the activation and the deactivation reaction can happen in their microscopic reverse direction, which corrupts the coding. Energy is needed to break time reversibility and protect the coding. Furthermore, for time-varying signals, we

also need to recognize that the samples correspond to the ligand concentration over the past integration time τ_r , which will in general differ from the current concentration L that the cell aims to estimate. While a finite τ_r is necessary for time integration, it will also lead to a systematic error in the estimate of the concentration that the cell cannot reduce by taking more receptor samples.

Estimating concentration from p_{τ_r} is no different from that via readout x^* Because the average number of samples \bar{N} is a constant, it follows from Eq. 7 that the variance in x^* given an input L is $\sigma_{x^*|L}^2 = \sigma_{\hat{p}_{\tau_r|L}}^2 \bar{N}^2$ while the gain from L to x^* is $\tilde{g}_{L \rightarrow x^*} = \tilde{g}_{L \rightarrow p_{\tau_r}} \bar{N}^2$. Consequently, the absolute error $(\delta\hat{L})^2$ in estimating the concentration via x^* , $(\delta\hat{L})^2 = \sigma_{x^*|L}^2 / \tilde{g}_{L \rightarrow x^*}^2$, is the same as that of Eq. 5: because the instantaneous number of active readout molecules x^* reflects the average receptor occupancy p_{τ_r} over the past τ_r , estimating the ligand concentration from x^* is no different from inferring it from the average receptor occupancy $\hat{p}_{\tau_r|L} = x^* / \bar{N}$. In the *Supporting Information* we show explicitly that the central result of our manuscript that follows from the sampling framework, Eq. 20, is indeed identical to that of Eq. 4 (section S-IV).

Key steps derivation central result We now sketch the derivation of the central result for a simpler system, the irreversible network ($k_{-f} = k_{-r} = 0$). For details and the result on the full system, see *SI*.

Dynamic gain The dynamic gain $\tilde{g}_{L \rightarrow p_{\tau_r}} = \delta p_{\tau_r} / \delta L(t)$ quantifies the mapping between the deviation $\delta L(t) \equiv L(t) - \bar{L}$ of the current ligand concentration $L(t)$ from its mean \bar{L} and the deviation δp_{τ_r} of the average receptor occupancy over the past integration time τ_r from its mean p , see Fig. 2(a). This average is taken by the readout molecules at time t . Taking into account deactivation, the probability that a readout molecule at time t provides a sample of the receptor at an earlier time t_i is $p(t_i|\text{sample}) = e^{-(t-t_i)/\tau_r} / \tau_r$ [12]. Averaging the receptor occupancy over the sampling times t_i then yields

$$\delta p_{\tau_r} = \int_{-\infty}^t dt_i \langle \delta n(t_i) \rangle_{\delta L(t)} \frac{e^{-(t-t_i)/\tau_r}}{\tau_r}. \quad (8)$$

Here, $\langle \delta n(t_i) \rangle_{\delta L(t)} = \langle n(t_i) \rangle_{\delta L(t)} - p$ is the average deviation in the receptor occupancy $n(t_i) = 0, 1$ at time t_i given that the ligand concentration at time t is $\delta L(t)$, where the average is taken over receptor-ligand binding noise and the subensemble of ligand trajectories that each end at $\delta L(t)$ (see Fig. 2c). We can compute it within the linear-noise approximation:

$$\langle \delta n(t_i) \rangle_{\delta L(t)} = \rho_n \int_{-\infty}^{t_i} dt' \langle \delta L(t') \rangle_{\delta L(t)} e^{-(t_i-t')/\tau_c}, \quad (9)$$

where $\rho_n = p(1-p)/(\bar{L}_T \tau_c)$ and $\langle \delta L(t') \rangle_{\delta L(t)}$ is the average ligand concentration at time t' given that the concentration at time t is $\delta L(t)$. It is given by [30]

$$\langle \delta L(t') \rangle_{\delta L(t)} = \delta L(t) e^{-|t-t'|/\tau_L}. \quad (10)$$

Combining Eqs. 8-10 yields

$$\tilde{g}_{L \rightarrow p_{\tau_r}} = \frac{p(1-p)}{\bar{L}} \left(1 + \frac{\tau_c}{\tau_L}\right)^{-1} \left(1 + \frac{\tau_r}{\tau_L}\right)^{-1}, \quad (11)$$

$$= g_{L \rightarrow p} \left(1 + \frac{\tau_c}{\tau_L}\right)^{-1} \left(1 + \frac{\tau_r}{\tau_L}\right)^{-1}. \quad (12)$$

The dynamic gain $\tilde{g}_{L \rightarrow p_{\tau_r}}$ depends on all the timescales in the problem. Only when $\tau_L \gg \tau_r, \tau_c$ is the average ligand concentration over the subensemble of trajectories ending at $\delta L(t)$ equal to current concentration $\delta L(t)$ (see Fig. 2(c)), and does $\tilde{g}_{L \rightarrow p_{\tau_r}}$ become equal to its maximal value, the static gain $g_{L \rightarrow p} = p(1-p)/\bar{L}$.

The error in estimating the receptor occupancy

Using the law of total variance, the error $\sigma_{\hat{p}_{\tau_r}|L}^2$ in the estimate of the receptor occupancy p_{τ_r} over the past integration time τ_r is given by

$$\sigma_{\hat{p}_{\tau_r}|L}^2 = \text{var} [E(\hat{p}_{\tau_r}|L|N)] + E [\text{var}(\hat{p}_{\tau_r}|L|N)]. \quad (13)$$

The first term reflects the variance of the mean of $\hat{p}_{\tau_r}|L$ given the number of samples N ; the second term reflects the mean of the variance in $\hat{p}_{\tau_r}|L$ given the number of samples N [12].

The first term of Eq. 13 is given by (see Eq. S48)

$$\text{var} [E(\hat{p}_{\tau_r}|L|N)] = \frac{p^2}{N}. \quad (14)$$

This contribution reflects the fact that with a push-pull network as considered here, the cell cannot discriminate between those readout molecules that have collided with an unbound receptor, and hence provide a sample of the receptor, and those that have not collided with a receptor at all; this term is zero for a bifunctional kinase where the unbound receptor catalyzes readout deactivation [12].

The second term of Eq. 13 contains two contributions. First we note that (Eq. S50 and Appendix S-B)

$$\begin{aligned} & \text{var} \left(\frac{\sum_{i=1}^N n_i(t_i)}{N} \middle| N \right) \\ &= \frac{p(1-p)}{N} + \overline{E\langle \delta n_i(t_i) \delta n_j(t_j) \rangle_{\delta L(t)}} - \tilde{g}^2 \sigma_L^2, \end{aligned} \quad (15)$$

where $\delta n_i(t_i) = n_i(t_i) - p$, E denotes an average over the sampling times t_i , and the overline an average over δL . The receptor covariance $\overline{E\langle \delta n_i(t_i) \delta n_j(t_j) \rangle_{\delta L(t)}}$ can be decomposed into two contributions. The first combines with the first term of Eq. 15 to yield (Eq. S61)

$$E [\text{var}(\hat{p}_{\tau_r}|L|N)]^{\text{samp}} = \frac{p(1-p)}{\bar{N}_I}, \quad (16)$$

where $\bar{N}_I = f_I \bar{N}$. Here, $f_I = 1/(1 + 2\tau_c/\Delta)$, with τ_c the receptor-ligand correlation time and Δ the spacing between the receptor samples, is the fraction of the \bar{N} samples that are independent. Eq. 16 is the error in the estimate of the receptor occupancy based on a single measurement—the variance of the receptor occupancy $p(1-p)$ —divided by the total number of independent measurements, $\bar{N}_I = f_I \bar{N}$. Together with the first term of Eq. 13 (i.e. Eq. 14) Eq. 16 yields the sampling error in the estimate of the average receptor occupancy over τ_r :

$$\sigma_{\hat{p}_{\tau_r}|L}^{2, \text{samp}} = \frac{p^2}{N} + \frac{p(1-p)}{\bar{N}_I}. \quad (17)$$

Both contributions to $\sigma_{\hat{p}_{\tau_r}|L}^{2, \text{samp}}$ are governed by the nature of the receptor sampling process and do not depend on the input statistics. They are indeed the same as those for sensing static concentrations, derived previously [12].

The second contribution to Eq. 13 comes from the second contribution to $\overline{E\langle \delta n_i(t_i) \delta n_j(t_j) \rangle_{\delta L(t)}}$ in Eq. 15. It combines with the third term of Eq. 15 to yield (see Eq. S72)

$$\begin{aligned} \sigma_{\hat{p}_{\tau_r}|L}^{2, \text{dyn}} &= E [\text{var}(\hat{p}_{\tau_r}|L|N)]^{\text{dyn}} \\ &= \tilde{g}^2 \sigma_L^2 \left[\left(1 + \frac{\tau_c}{\tau_L}\right) \left(1 + \frac{\tau_r}{\tau_L}\right) \left(1 + \frac{\tau_c \tau_r}{\tau_L(\tau_c + \tau_r)}\right) - 1 \right] \end{aligned} \quad (18)$$

This is the dynamical error in estimating p_{τ_r} . It corresponds to the variation in p_{τ_r} that arises from the different concentration trajectories in the past τ_r that each end at $\delta L(t)$, see Fig. 2(c). This error does depend on the statistics of the input signal: it increases with the width of the input distribution, σ_L^2 , and decreases with the input timescale τ_L .

The error in estimating the average receptor occupancy p_{τ_r} is then given by

$$\sigma_{\hat{p}_{\tau_r}|L}^2 = \sigma_{\hat{p}_{\tau_r}|L}^{2, \text{samp}} + \sigma_{\hat{p}_{\tau_r}|L}^{2, \text{dyn}}, \quad (19)$$

where $\sigma_{\hat{p}_{\tau_r}|L}^{2, \text{samp}}$ and $\sigma_{\hat{p}_{\tau_r}|L}^{2, \text{dyn}}$ are given by Eqs. 17 and 18.

Central result To know how the error $\sigma_{\hat{p}_{\tau_r}|L}^2$ in the estimate of the average receptor occupancy p_{τ_r} propagates to the error $(\delta \hat{L})^2$ in the estimate of the ligand concentration, we divide Eq. 19 by the dynamic gain $\tilde{g}_{L \rightarrow p_{\tau_r}}$ given by Eq. 11 (see Eq. 6). For the full system, the reversible push-pull network, this yields the central result of our manuscript, the signal-to-noise ratio in terms of the total number of receptor samples, their independence, their accuracy, and the timescale on which they are generated:

$$\text{SNR}^{-1} = \underbrace{\left(1 + \frac{\tau_c}{\tau_L}\right)^2 \left(1 + \frac{\tau_r}{\tau_L}\right)^2 \left[\frac{(\bar{L}/\sigma_L)^2}{p(1-p)\bar{N}_I} + \frac{(\bar{L}/\sigma_L)^2}{(1-p)^2\bar{N}_{\text{eff}}} \right]}_{\text{sampling error}} + \underbrace{\left(1 + \frac{\tau_c}{\tau_L}\right) \left(1 + \frac{\tau_r}{\tau_L}\right) \left(1 + \frac{\tau_c\tau_r}{\tau_L(\tau_c + \tau_r)}\right) - 1}_{\text{dynamical error}} \quad (20)$$

This expression represents exactly the same result as that obtained by the straightforward linear-noise calculation, Eq. 4 (section S-IV). However, it is much more illuminating. It shows that the sensing error SNR^{-1} can be decomposed into two distinct contributions, which each have a clear interpretation: the *sampling error*, arising from the stochasticity in the sampling of the receptor state, and the *dynamical error*, arising from the dynamics of the input signal.

When the timescale of the ligand fluctuations τ_L is much longer than the receptor correlation time τ_c and the integration time τ_r , $\tau_L \gg \tau_r, \tau_c$, the dynamical error reduces to zero and only the sampling error remains. In this limit, the prefactor $(1 + \tau_c/\tau_L)^2(1 + \tau_r/\tau_L)^2$ becomes unity, and the relative sensing error $(\delta\hat{L}/\bar{L})^2$ (instead of $\text{SNR}^{-1} = (\delta\hat{L}/\sigma_L)^2$) reduces to that of estimating *static* concentrations, derived previously in Ref. [12]. Here, \bar{N}_{eff} is the total number of effective samples and \bar{N}_I is the number of these that are independent [12]. For the full system they are given by:

$$\bar{N}_I = \underbrace{\frac{1}{(1 + 2\tau_c/\Delta)}}_{f_I} \underbrace{\frac{\overbrace{(e^{\beta\Delta\mu_1} - 1)(e^{\beta\Delta\mu_2} - 1)}^q}{e^{\beta\Delta\mu} - 1}}_{\bar{N}_{\text{eff}}} \underbrace{\frac{\overbrace{\dot{n}\tau_r}^N}{p}}. \quad (21)$$

The quantity $\dot{n} = k_f p R_T \bar{x} - k_{-f} p R_T \bar{x}^*$ is the net flux of x around the cycle of activation and deactivation. It equals the rate at which x is modified by the ligand-bound receptor; the quantity \dot{n}/p is thus the sampling rate of the receptor, be it ligand bound or not. Multiplied with the relaxation rate τ_r , it yields the total number of receptor samples \bar{N} obtained during τ_r . However, not all these samples are reliable. The effective number of samples is $\bar{N}_{\text{eff}} = q\bar{N}$, where $0 < q < 1$ quantifies the quality of the sample. Here, $\beta = 1/(k_B T)$ is the inverse temperature, $\Delta\mu_1$ and $\Delta\mu_2$ are the free-energy drops over the activation and deactivation reaction, respectively, with $\Delta\mu = \Delta\mu_1 + \Delta\mu_2$ the total drop, determined by the fuel turnover (see Fig. 1(b)). If the system is in thermodynamic equilibrium, $\Delta\mu_1 = \Delta\mu_2 = \Delta\mu = 0$, $q \rightarrow 0$ and the system cannot sense, while if the system is strongly driven and $\Delta\mu_1, \Delta\mu_2 \rightarrow \infty$, $q \rightarrow 1$ and $\bar{N}_{\text{eff}} \rightarrow \bar{N}$. Yet, even when all samples are reliable, they may contain redundant information on the receptor state. The factor f_I is the fraction of the \bar{N}_{eff} samples that are independent. It reaches unity when the receptor sampling interval $\Delta = 2\tau_r/(\bar{N}_{\text{eff}}/R_T)$ becomes larger than the receptor correlation time τ_c .

When the number of samples becomes very large and $\bar{N}_I, \bar{N}_{\text{eff}} \rightarrow \infty$, the sampling error reduces to zero. However, the sensing error still contains a second contribution, which, following Ref. [30], we call the dynamical error. This contribution only depends on timescales. It arises from the fact that the samples encode the receptor history and hence the ligand concentration over the past τ_r , which will, in general, deviate from the quantity that the cell aims to predict—the current concentration L . Indeed, this contribution yields a systematic error, which cannot be eliminated by increasing the number of receptor samples, their independence or their accuracy. It can only be reduced to zero by making the integration time τ_r much smaller than the ligand timescale τ_L (assuming that τ_c is typically much smaller than τ_r, τ_L). Only in this regime will the ligand concentration in the past τ_r be similar to the current concentration, and can the latter be reliably inferred from the occupancy of the receptor provided the latter has been estimated accurately by taking enough samples.

Importantly, the dynamics of the input signal not only affects the sensing precision via the dynamical error, but also via the sampling error. This effect is contained in the prefactor of the sampling error, $(1 + \tau_c/\tau_L)^2(1 + \tau_r/\tau_L)^2$, which has its origin in the dynamic gain $\tilde{g}_{L \rightarrow p_{\tau_r}}$ (Eq. 11). It determines how the sampling error $\sigma_{p_{\tau_r}|L}^{2, \text{samp}}$ in the estimate of p_{τ_r} (Eq. 17) propagates to the error in the estimate of L (see Eq. 6). Only when $\tau_c, \tau_r \ll \tau_L$ can the readout system closely track the input signal, and does $\tilde{g}_{L \rightarrow p_{\tau_r}}$ reach its maximal value, the static gain $g_{L \rightarrow p}$, thus minimizing the error propagation from p_{τ_r} to L .

III. FUNDAMENTAL RESOURCES

We can use Eq. 20 to identify the *fundamental* resources for cell sensing [12]. A fundamental resource is a (collective) variable Q_i that, when fixed to a constant, puts a non-zero lower bound on SNR^{-1} , no matter how the other variables are varied. It is thus mathematically defined as:

$$\text{MIN}_{Q_i = \text{const}} (\text{SNR}^{-1}) = f(\text{const}) > 0. \quad (22)$$

To find these collective variables, we numerically or analytically minimized SNR^{-1} , constraining (combinations of) variables yet optimizing over the other variables. To this end, it is helpful to rewrite Eq. 20 by splitting the first term in between the square brackets of the sampling error and then grouping one term with the second term using that $\bar{N}_{\text{eff}} = q\bar{N} = q\dot{n}\tau_r/p$ (see also section S-V):

$$\text{SNR}^{-1} = \left(1 + \frac{\tau_c}{\tau_L}\right)^2 \left(1 + \frac{\tau_r}{\tau_L}\right)^2 \left[\underbrace{\frac{(\bar{L}/\sigma_L)^2}{p(1-p)R_T(1+\tau_r/\tau_c)}}_{\text{receptor input noise}} + \underbrace{\frac{(\bar{L}/\sigma_L)^2}{(1-p)^2 q \dot{n} \tau_r}}_{\text{coding noise}} \right] + \underbrace{\left(1 + \frac{\tau_c}{\tau_L}\right) \left(1 + \frac{\tau_r}{\tau_L}\right) \left(1 + \frac{\tau_c \tau_r}{\tau_L(\tau_c + \tau_r)}\right)}_{\text{dynamical error}} - 1. \quad (23)$$

The first term in between the square brackets describes the contribution that comes from the stochasticity in the concentration measurements at the receptor level. The second term in between the square brackets, the coding noise, describes the error that arises in storing these measurements into the readout molecules.

Eq. 23 allows us to identify the fundamental resources by constraining combinations of variables while optimizing over others by taking limits (see Eq. 22). As we show below, this reveals that these resources are the number of receptors R_T , their integration time τ_r , the number of readout molecules X_T , and the power $\dot{w} = \dot{n}\Delta\mu$. Fig. 3 illustrates that these resources are indeed fundamental, and also elucidates the design logic of the system.

Panel (a) of Fig. 3 shows the maximal mutual information $I_{\max}(L; x^*)$ as a function of X_T for different values of R_T , obtained by optimizing Eq. 23 over p and τ_r , in the irreversible limit $q \rightarrow 1$. When X_T is small, I_{\max} cannot be increased by raising R_T : no matter how many receptors the system has, the sensing precision is limited by the pool of readout molecules and only increasing this pool can raise I_{\max} . However, when X_T is large, I_{\max} becomes independent of X_T . In this regime, the number of receptors R_T limits the number of independent concentration measurements and only increasing R_T can raise I_{\max} . Similarly, panel (b) shows that when the power \dot{w} is limiting, I_{\max} cannot be increased by R_T but only by increasing \dot{w} . Clearly, the resources receptors, readout molecules and energy cannot compensate each other: the sensing precision is bounded by the limiting resource.

Importantly, however, while for sensing static concentrations the products $R_T\tau_r/\tau_c$ (receptors and their integration time) and $\dot{w}\tau_r$ (the energy) are fundamental [12], for time-varying signals R_T , \dot{w} , and τ_r separately limit sensing. Consequently, neither receptors R_T nor power \dot{w} can be traded freely against time τ_r to reach a desired sensing precision, as is possible for static signals. There exists an optimal integration time τ_r^{opt} that maximizes the sensing precision, and its value depends on which of the resources R_T , X_T and \dot{w} is limiting (Fig. 3(c)-(f)). We now discuss these three regimes in turn.

A. The number of receptors R_T

As Berg and Purcell pointed out, cells can reduce the sensing error by increasing the number of receptors or by taking more measurements per receptor, via the mecha-

nism of time integration [1]. In the *Berg-Purcell* regime where the receptors and their integration time are limiting, the coding noise is zero and Eq. 23 reduces to

$$\text{SNR}^{-1} \geq \left(1 + \frac{\tau_r}{\tau_L}\right)^2 \frac{4(\bar{L}/\sigma_L)^2}{R_T \tau_r/\tau_c} + \frac{\tau_r}{\tau_L}. \quad (24)$$

This result corresponds to the limits $X_T \rightarrow \infty$ and $\dot{w} \rightarrow \infty$ in panels (a) and (b) of Fig. 3, respectively.

Eq. 24 shows that the sensing precision does not depend on $R_T\tau_r/\tau_c$, as for static signals [12], but on R_T and τ_r separately, such that an optimal integration time τ_r^{opt} emerges that maximizes the sensing precision (see Fig. 3c). Increasing τ_r improves the mechanism of time integration by increasing the number of independent samples per receptor, τ_r/τ_c , thus reducing the sampling error (Eq. 20). However, increasing τ_r raises the dynamical error. Moreover, it lowers the dynamical gain $\tilde{g}_{L \rightarrow p\tau_r}$, which increases the propagation of the error in the estimate of the receptor occupancy to that of the ligand concentration. The optimal integration time τ_r^{opt} arises as a trade-off between these three factors.

Fig. 3(c) also shows that the optimal integration time τ_r^{opt} decreases with the number of receptors R_T . The total number of independent concentration measurements is the number of independent measurements per receptor, τ_r/τ_c , times the number R_T of receptors, $\bar{N}_I = R_T\tau_r/\tau_c$. As R_T increases, less measurements τ_r/τ_c per receptor have to be taken to remove the receptor-ligand binding noise, explaining why τ_r^{opt} decreases as R_T increases. Indeed, the sensing error reduces to zero when $R_T \rightarrow \infty$ and $\tau_r \rightarrow 0$, allowing for optimal signal tracking.

Interestingly, τ_r^{opt} depends non-monotonically on the receptor-ligand correlation time τ_c (Fig. 3d). When τ_c increases at fixed τ_r , the receptor samples become more correlated. To keep the mechanism of time integration effective, τ_r must increase as τ_c rises. Increasing τ_r will, however, also distort the signal, and to avoid too strong signal distortion the cell compromises on time integration by decreasing the *ratio* τ_r/τ_c (see inset). When τ_r becomes too large, the benefit of time integration no longer pays off the cost of signal distortion. Now not only the ratio τ_r/τ_c decreases (inset of Fig. 3(d)), but also τ_r itself (Fig. 3(c)). The sensing system switches to a different strategy. It no longer employs time integration, but rather becomes an instantaneous responder of the ligand-binding state of the receptor.

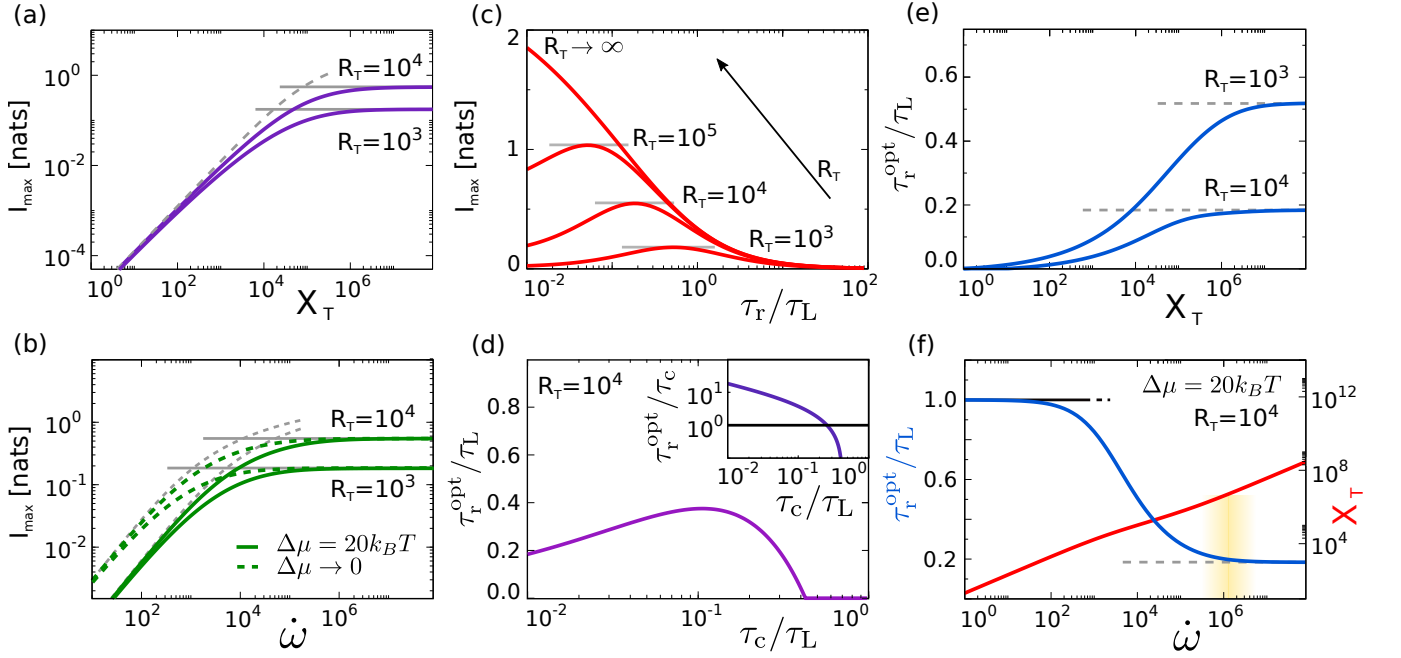


FIG. 3. **Receptors R_T , readout molecules X_T and \dot{w} fundamentally limit sensing, and there exists an optimal integration time τ_r that depends on which of the resources is limiting.** (a+b) R_T , X_T and \dot{w} are fundamental resources, with no trade-offs between them. Plotted is the maximum mutual information $I_{\max} = 1/2 \ln(1 + \text{SNR}_{\max})$, obtained by minimizing Eq. 23 over p and τ_r , for different combinations of (a) X_T and R_T in the irreversible limit $q \rightarrow 1$, and (b) \dot{w} and R_T for two different values of $\Delta\mu$. The sensing precision is bounded by the limiting resource, R_T (solid grey lines, Eq. 24), X_T (dashed grey line, Eq. 25, panel a), or \dot{w} (dashed grey lines, Eqs. 27 and 28, panel b). (c) I_{\max} as a function of τ_r for different values of R_T in the Berg-Purcell limit ($q \rightarrow 1$ and $X_T \rightarrow \infty$). There exists an optimal integration time τ_r^{opt} that maximizes the sensing precision; τ_r^{opt} decreases with R_T . (d) In this limit, τ_r^{opt} depends non-monotonically on the receptor-ligand correlation time τ_c : it first increases with τ_c to sustain time-averaging, but then drops when $\tau_r^{\text{opt}}/\tau_c$ becomes of order unity and time-averaging is no longer effective (see inset). (e) τ_r^{opt} as a function of X_T for different values of R_T . When $X_T < R_T$, time averaging is not possible and the optimal system is an instantaneous responder, $\tau_r^{\text{opt}} \rightarrow 0$; when $X_T \gg R_T$ the system reaches the Berg-Purcell regime in which I_{\max} is limited by R_T rather than X_T (see panel a). (f) τ_r^{opt} and X_T as a function of \dot{w} . When the power $\dot{w} \sim X_T/\tau_r$ is limiting, the sampling error dominates and τ_r^{opt} equals τ_L to maximize X_T , minimizing the sampling error; τ_r^{opt} then decreases to trade part of the decrease in the sampling error for a reduction in the dynamical error such that both decrease; when the sampling interval $\Delta \sim \tau_r R_T/X_T$ becomes comparable to τ_c , in the region marked by the yellow bar, the sampling error is no longer limited by X_T , such that τ_r now limits both sources of error; the two sources can therefore no longer be decreased simultaneously by increasing $\dot{w} \sim X_T/\tau_r$; the system has entered the Berg-Purcell regime where τ_r^{opt} is determined by R_T rather than \dot{w} (see panel (b)). Parameter values unless specified: $\tau_c/\tau_L = 10^{-2}$; $\sigma_L/\bar{L}_T = 10^{-2}$.

B. The number of readout molecules X_T

To implement time integration, the cell needs to store the receptor states in the readout molecules. When the number of readout molecules X_T is limiting, the coding noise in Eq. 23 dominates over the receptor input noise. Noting that the flux $\dot{n} = f(1-f)qX_T/\tau_r$, with $f = \bar{x}^*/X_T$ the fraction of modified readout molecules, we find that in the irreversible regime ($q \rightarrow 1$), the sensing error is bounded by

$$\text{SNR}^{-1} \geq \left(1 + \frac{\tau_r}{\tau_L}\right)^2 \left[\frac{4(\bar{L}/\sigma_L)^2}{X_T} \right] + \frac{\tau_r}{\tau_L} \quad (25)$$

$$\geq \frac{4(\bar{L}/\sigma_L)^2}{X_T}. \quad (26)$$

Clearly, X_T is a fundamental resource that puts a hard bound on the mutual information (Fig. 3(a)).

Eqs. 25 and 26 show that to reach the sensing limit set by X_T , the receptor integration time τ_r needs to be zero. This is in marked contrast to the non-zero optimal integration τ_r^{opt} in the Berg-Purcell regime where R_T is limiting (see Fig. 3(c)). To elucidate this, Fig. 3(e) shows the optimal integration time τ_r^{opt} as a function of X_T . When X_T is smaller than R_T , the average number of samples per receptor is less than unity. At any given time, there are many receptors whose concentration measurements are not stored in the downstream readout molecules. In this regime, the system cannot time integrate the receptor, and to minimize signal distortion the optimal integration time τ_r^{opt} is essentially zero. However, when X_T is increased, the likelihood that two or

more readout molecules provide a sample of the same receptor molecule rises, and time averaging becomes possible. Yet to obtain receptor samples that are independent, the integration time τ_r must be increased to make the sampling interval $\Delta \sim \tau_r R_T / X_T$ larger than the receptor correlation time τ_c . As X_T and hence the total number of samples \bar{N} are increased further, the number of samples that are independent, \bar{N}_I , only continues to rise when τ_r increases with X_T further. However, while this reduces the sampling error, it does also increase the dynamical error. When the decrease in the sampling error no longer outweighs the increase in the dynamical error, τ_r^{opt} and the mutual information no longer change with X_T (see Fig. 3(a)). The system has entered the Berg-Purcell regime in which τ_r^{opt} and the mutual information are given by the optimization of Eq. 24 (grey dashed line). In this regime, increasing X_T merely adds redundant samples: the number of independent samples remains $\bar{N}_I = R_T \tau_r^{\text{opt}} / \tau_c$.

C. The power $\dot{w} = \dot{n}\Delta\mu$

Time integration relies on copying the ligand-binding state of the receptor into the chemical modification states of the readout molecules [10, 12]. This copy process correlates the state of the receptor with that of the readout, which requires work input [32].

The free-energy $\Delta\mu$ provided by the fuel turnover drives the readout around the cycle of modification and demodification (Fig. 1). The rate at which the fuel molecules do work is the power $\dot{w} = \dot{n}\Delta\mu$ and the total work performed during the integration time τ_r is $w \equiv \dot{w}\tau_r$. This work is spent on taking samples of receptor molecules that are bound to ligand, because only they can modify the readout. The total number of effective samples of ligand-bound receptors during τ_r is $p\bar{N}_{\text{eff}}$ (Eq. 21), which means that the work per effective sample of a ligand-bound receptor is $w/(p\bar{N}_{\text{eff}}) = \Delta\mu/q$ [12].

To understand how energy limits the sensing precision, we can distinguish between two limiting regimes [12]. When $\Delta\mu > 4k_B T$, the quality factor $q \rightarrow 1$ (Eq. 21) and the work per sample of a ligand-bound receptor is simply $w/(p\bar{N}_{\text{eff}}) = \Delta\mu$ [12]. In this irreversible regime, the power limits the sensing accuracy not because it limits the reliability of each sample, but because it limits the rate $\dot{n} = \dot{w}/\Delta\mu$ at which the receptor is sampled:

$$\text{SNR}^{-1} \geq \left(1 + \frac{\tau_r}{\tau_L}\right)^2 \left(\frac{\Delta\mu (\bar{L}/\sigma_L)^2}{\dot{w}\tau_r}\right) + \frac{\tau_r}{\tau_L}, \quad (27)$$

obtained from Eq. 23 by taking $R_T \rightarrow \infty$, $p \rightarrow 0$. This expression shows that the sensing precision is fundamentally bounded not by the work $w = \dot{w}\tau_r$, as observed for static signals [12], but rather by the power \dot{w} and the integration time τ_r separately such that an optimal integration time τ_r^{opt} emerges (Fig. 3(f)).

When $\Delta\mu < 4k_B T$, the system enters the quasi-equilibrium regime in which the quality factor $q \rightarrow \beta\Delta\mu/4$ (see Eq. 21, noting that in the optimal system $\Delta\mu_1 = \Delta\mu_2 = \Delta\mu/2$) [12]. The bound on the sensing error (Eq. 23) set by the power constraint now becomes

$$\text{SNR}^{-1} \geq \left(1 + \frac{\tau_r}{\tau_L}\right)^2 \left(\frac{4k_B T (\bar{L}/\sigma_L)^2}{\dot{w}\tau_r}\right) + \frac{\tau_r}{\tau_L}. \quad (28)$$

Comparing this expression to Eq. 27, which only holds when $\Delta\mu > 4k_B T$, it is clear that the sensing error is minimized in the quasi-equilibrium regime, see Fig. 3(b). This regime maximizes the number of effective measurements per work input, because the work per effective measurement reaches its fundamental lower bound, $w/(p\bar{N}_{\text{eff}}) = \Delta\mu/q = 4k_B T$ [12].

While the sensing precision for a given power and time constraint is higher in the quasi-reversible regime, more readout molecules are required to store the concentration measurements in this regime. Noting that the flux $\dot{n} = f(1-f)X_T q/\tau_r = \dot{w}/\Delta\mu$ (Eq. S114), it follows that in the irreversible regime ($q \rightarrow 1$) the number of readout molecules consuming energy at a rate \dot{w} is

$$X_T^{\text{irr}} = \frac{\dot{w}\tau_r}{\Delta\mu f(1-f)} \quad (29)$$

while in the quasi-equilibrium regime ($q \rightarrow \Delta\mu/4$) it is

$$X_T^{\text{qeq}} = \frac{\dot{w}\tau_r 4k_B T}{\Delta\mu^2 f(1-f)}. \quad (30)$$

Since in the quasi-equilibrium regime $\Delta\mu < 4k_B T$, $X_T^{\text{qeq}} > X_T^{\text{irr}}$.

Fig. 3(f) shows how the optimal integration time τ_r^{opt} depends on the power \dot{w} . Since the system cannot sense without any readout molecules, in the low power regime the system maximizes X_T subject to the power constraint $\dot{w} \sim X_T/\tau_r$ (see Eqs. 29 and 30) by making τ_r as large as possible, which is the signal correlation time τ_L —increasing τ_r^{opt} further would average out the signal itself. As \dot{w} is increased, X_T rises and the sampling error decreases. When the sampling error becomes comparable to the dynamical error (Eq. 20), the system starts to trade a further reduction in the sampling error for a reduction in the dynamical error: τ_r^{opt} now goes down. In this regime, the sampling error and the dynamical error are reduced simultaneously by increasing X_T and decreasing τ_r^{opt} . This continues until the sampling interval $\Delta \sim R_T \tau_r / X_T$ becomes comparable to the receptor correlation time τ_c , as marked by the yellow bar. Beyond this point, $\Delta < \tau_c$ and the sampling error is no longer limited by X_T but rather by τ_r , since τ_r bounds the number of independent samples per receptor, τ_r/τ_c . Because τ_r now limits both sources of error, they can no longer be reduced simultaneously. The system has entered the Berg-Purcell regime, where τ_r^{opt} is determined by the trade-off between the dynamical error and the sampling error as set by the maximum number of independent samples, $R_T \tau_r / \tau_c$ (Fig. 3(c)).

IV. THE OPTIMAL ALLOCATION PRINCIPLE, REVISITED

In sensing static concentrations, there exists three fundamental classes of resources: receptors and their integration time $R_T\tau_r/\tau_c$, readout molecules X_T , and energy $\dot{w}\tau_r$ injected during τ_r [12]. These fundamental resource classes cannot compensate each other in achieving a desired sensing precision—they limit sensing like weak links in a chain. It means that in an optimally designed system each class is equally limiting so that no resource is wasted. This yields the design principle that in an optimal system $R_T\tau_r/\tau_c \approx X_T \approx \beta\dot{w}\tau_r$ [12]. However, in sensing time-varying signals, a trade-off between time integration and signal tracking is inevitable. As a result, besides X_T , the receptors R_T , the power \dot{w} and the integration time τ_r are each fundamental.

Can we nonetheless formulate a similar design principle? We cannot simply equate the bounds set by the number of receptors R_T and their integration time τ_r (Eq. 24), the number of readout molecules X_T (Eq. 26) and the power \dot{w} (Eq. 28), because they correspond to different sensing strategies: when R_T is limiting, there exists an optimal non-zero integration time τ_r^{opt} , while if X_T is limiting $\tau_r^{\text{opt}} \approx 0$, as discussed above.

Remarkably, however, Eqs. 24, 25 and 28 have the same functional form $f(x)$, with $x = R_T\tau_r/\tau_c, X_T, \beta\dot{w}\tau_r$, respectively. This means that when for a given τ_r , $R_T\tau_r/\tau_c = X_T = \beta\dot{w}\tau_r$ and $f(R_T\tau_r/\tau_c) = f(X_T) = f(\beta\dot{w}\tau_r)$, the bounds on the sensing precision as set by, respectively, the number of receptors R_T (Eq. 24), the number of readout molecules X_T (Eq. 25), and the power \dot{w} (Eq. 28), are equal. Each of these resources is now equally limiting sensing and no resource is in excess. We thus recover the optimal resource allocation principle originally formulated for systems sensing static concentrations [12]:

$$R_T\tau_r/\tau_c \approx X_T \approx \beta\dot{w}\tau_r. \quad (31)$$

Irrespective of whether the concentration fluctuates in time, the number of independent concentration measurements at the receptor level is $R_T\tau_r/\tau_c$, which in an optimally designed system also equals the number of readout molecules X_T and the energy $\beta\dot{w}\tau_r$ that are both necessary and sufficient to store these measurements reliably.

Importantly, Eq. 31 holds for any integration time τ_r , yet it does not specify τ_r . What is the optimal τ_r that minimizes the sensing error? The design principle $R_T\tau_r/\tau_c = X_T$ means that for a fixed X_T , R_T can be increased by simultaneously decreasing τ_r . This increases the sensing precision (see Fig. S1, S-VII). In fact, for a fixed X_T , the precision is maximized when $R_T = X_T$ and $\tau_r = 0$, because in this limit the dynamical error is zero. However, the power diverges in this limit, because in the optimal system $\beta\dot{w}\tau_r \approx X_T$ (Eq. 31).

Intriguingly, the cell membrane is highly crowded and many systems employ time integration [1, 4, 12]. This suggests that these systems employ time integration and accept the signal distortion that comes with it, simply

because there is not enough space on the membrane to increase R_T . Our theory then allows us to predict the optimal integration time τ_r^{opt} based on the premise that R_T is limiting. As Eq. 24 reveals, in this limit τ_r^{opt} does not only depend on R_T , but also on τ_c , τ_L , and σ_L/\bar{L} : $\tau_r^{\text{opt}} = \tau_r^{\text{opt}}(R_T, \tau_c, \tau_L, \sigma_L/\bar{L})$. The optimal design of the system is then given by Eq. 31 but with τ_r given by $\tau_r^{\text{opt}} = \tau_r^{\text{opt}}(R_T, \tau_c, \tau_L, \sigma_L/\bar{L})$:

$$R_T\tau_r^{\text{opt}}/\tau_c \approx X_T^{\text{opt}} \approx \beta\dot{w}^{\text{opt}}\tau_r^{\text{opt}}. \quad (32)$$

This design principle maximizes for a given number of receptors R_T the sensing precision, and minimizes the number of readout molecules X_T and power \dot{w} needed to reach that precision.

V. COMPARISON WITH EXPERIMENTS

If the number of receptors is limiting the sensing precision, then our theory predicts an optimal integration time $\tau_r^{\text{opt}}(R_T, \tau_c, \tau_L, \sigma_L/\bar{L})$ that is given by Eq. 24. We can test this prediction for the chemotaxis system of the bacterium *E. coli*, which has been well characterized experimentally. In this system, the receptor forms a complex with the kinase CheA. This complex, which can be coarse-grained into R [12], can bind the ligand L and activate the intracellular messenger protein CheY (x) by phosphorylating it. Deactivation of CheY is catalyzed by CheZ, the effect of which can be coarse-grained into the deactivation rate. The *E. coli* chemotaxis system also exhibits adaptation on longer timescales, due to receptor methylation and demethylation. However, the integration time for the receptor-ligand binding noise is not given by the adaptation timescale, but rather by the relaxation rate of the push-pull network that controls CheY (de) phosphorylation [21].

To test the prediction for $\tau_r^{\text{opt}}(R_T, \tau_c, \tau_L, \sigma_L/\bar{L})$, we need to estimate R_T , τ_c , τ_L and σ_L/\bar{L} . The number of receptor-CheA complexes depends on the growth rate and varies between $R_T = 10^3$ and $R_T = 10^4$ [33]. The dissociation constant for the binding of aspartate to the Tar receptor is $K_D \approx 0.1\mu\text{M}$ [34], which with an association rate of $k_{\text{on}} \approx 10^9\text{M}^{-1}/\text{s}$ [35] yields a receptor-ligand dissociation rate of $k_{\text{off}} \approx 100\text{s}^{-1}$. Protein occupancies are typically in the range 0.1 – 1 and following our previous work we assume $p = 0.5$ [12], which gives a receptor-ligand correlation time of $\tau_c \simeq 1/(2k_{\text{off}}) \approx 10\text{ms}$. The timescale τ_L of the input fluctuations is set by the typical run time, which is on the order of a few seconds, $\tau_L \approx 1\text{s}$ [36, 37].

This leaves one important parameter to be determined, the relative variance of the ligand concentration fluctuations, $(\sigma_L/\bar{L})^2$. This is set by the spatial ligand concentration profile and by the typical length of a run. We have a good estimate of the latter; in shallow gradients it is on the order of $l \simeq 50\mu\text{m}$ [36–39]. However, we do not know the spatial concentration profiles that *E. coli* has experienced during its evolution. For this

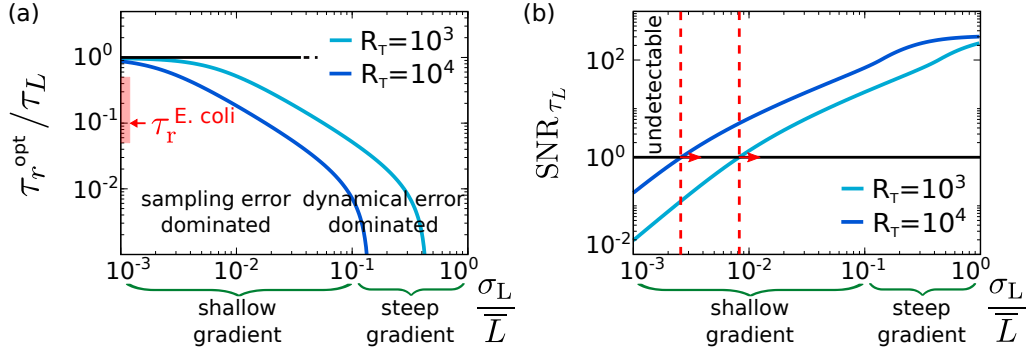


FIG. 4. **The optimal integration time for the chemotaxis system of *E. coli*.** (a) The optimal integration time τ_r^{opt} , obtained by numerically optimizing Eq. 24, as a function of the relative strength of the input noise, σ_L / \bar{L} , for two different copy numbers R_T of the receptor-CheA complexes; for an exponential gradient with length scale x_0 , the relative noise strength $\sigma_L / \bar{L} \simeq l / x_0$, where $l \approx 50 \mu\text{m}$ is the run length of *E. coli*. It is seen that τ_r^{opt} increases as σ_L / \bar{L} decreases. This is because the relative importance of the sampling error compared to the dynamical error increases, necessitating a longer integration time. The figure also shows that τ_r^{opt} decreases as R_T is increased, because that allows for more instantaneous measurements (see also Fig. 3). The red bar indicates the range of the estimated integration time of *E. coli*, $0.05\text{ms} < \tau_r < 0.5\text{ms}$, based on its attractant and repellent response respectively [41], divided by the input timescale $\tau_L \approx 1\text{s}$ based on its typical run time of about a second [36, 37]. The panel indicates that *E. coli* has been optimized to detect shallow concentration gradients. (b) The signal-to-noise ratio $\text{SNR}_{\tau_L} = (\sigma_L / \delta \hat{L})^2 \tau_L / \tau_r$ as a function of $\sigma_L / \bar{L} \simeq l / x_0$. To be able to detect the gradient, the SNR_{τ_L} must exceed unity. The panel shows that the shallowest gradient that *E. coli* can detect (marked with dashed red line) has, for $R_T = 10^4$, a length scale of $x_0 \approx 25000 \mu\text{m}$ (corresponding to $\sigma_L / \bar{L} \approx 2 \times 10^{-3}$), which is consistent with experiments based on ramp responses [40]. Other parameter: receptor-ligand binding correlation time $\tau_c = 10\text{ms}$ [34, 35].

reason we will study the optimal integration time as a function of $(\sigma_L / \bar{L})^2$. We can however get a sense of the scale by considering an exponential ligand-concentration gradient. For a profile $\bar{L}(x) = L_0 e^{x/x_0}$ with length scale x_0 , the relative change in the signal over the length of a run is $\sigma_L / \bar{L} \simeq (d\bar{L}/dx)l / \bar{L} = l / x_0$. Experiments indicate that for $x_0 \gtrsim 500 \mu\text{m}$ the cells reach a stable drift velocity before the receptor saturates [39, 40]. Inspired by these observations, we consider the range $\sigma_L / \bar{L} \approx l / x_0 < 1$, where $\sigma_L / \bar{L} < 0.1$ corresponds to shallow gradients with $x_0 \gtrsim 500 \mu\text{m}$ in which the cells move with a constant speed [39, 40].

Fig. 4 shows the result. Panel (a) shows that as the gradient becomes steeper and $\sigma_L / \bar{L} \approx l / x_0$ increases, the optimal integration time τ_r^{opt} decreases, dropping to zero when $\sigma_L / \bar{L} > 0.1$. We can understand the qualitative behavior by noting that the relative importance of the dynamical error as compared to the sampling error scales with $(\sigma_L / \bar{L})^2$ (see Eq. 24). Hence, when the gradient is shallow and σ_L / \bar{L} is small, the dynamical error is small compared to the sampling error, which allows for a larger optimal integration time τ_r^{opt} ; at the same time, our theory predicts that τ_r^{opt} depends on the input timescale τ_L , such that even in very shallow gradients τ_r^{opt} is bounded by τ_L . In contrast, in steep gradients, σ_L / \bar{L} and hence the dynamical error will be large, which necessitates a small τ_r^{opt} . In fact, for $\sigma_L / \bar{L} > 0.1$, the optimal system is an instantaneous responder.

Experiments indicate that the relaxation rate of CheY is $\tau_r^{-1} \approx 2\text{s}^{-1}$ for the attractant response and $\approx 20\text{s}^{-1}$ for the repellent response [41], such that the integration time $\tau_r \approx 50 - 500\text{ms}$ [12, 41]. Fig. 4(a) shows

that, according to our theory, this integration time is optimal for detecting shallow gradients, in the range $l / x_0 \approx \sigma_L / \bar{L} \approx 10^{-3} - 10^{-1}$. Our theory thus suggests that the sensing system of *E. coli* has been optimized for sensing shallow gradients.

While Fig. 4 indicates that the sensing system of *E. coli* has been optimized for detecting shallow gradients, it does not tell us whether cells can actually do so. To navigate, the cells must be able to resolve the signal change over a run. This means that the signal-to-noise ratio SNR_{τ_L} for the concentration measurements during a run of duration τ_L must at least be of order unity. If the SNR_{τ_L} is close to unity, it indicates that the system operates close to its fundamental sensing limits.

The signal change over a run is $\sigma_{\tau_L}^2$ and the effective error $(\delta \hat{L})^2 / (\tau_L / \tau_r)$ on the concentration measurements during a run is the instantaneous sensing error $(\delta \hat{L})^2$ divided by the number of independent concentration measurement τ_L / τ_r taken during a run of duration τ_L . The signal-to-noise ratio for these measurements is thus $\text{SNR}_{\tau_L} \equiv (\sigma_L / \delta \hat{L})^2 \tau_L / \tau_r$. It is plotted in Fig. 4(b) for the optimized system, with τ_r equal to the optimal integration time τ_r^{opt} that maximizes the sensing precision, given by Eq. 24.

Fig. 4 shows that our theory predicts that when $R_T = 10^3$, the shallowest gradient that cells can resolve, defined by $\text{SNR}_{\tau_L} = 1$, is $l / x_0 \approx \sigma_L / \bar{L} \approx 1 \times 10^{-2}$, corresponding to $x_0 \approx 7500 \mu\text{m}$, while when $R_T = 10^4$, it is $l / x_0 \approx 2 \times 10^{-3}$ corresponding to $x_0 \approx 25000 \mu\text{m}$; the shallowest gradient is thus on the order of $x_0 \approx 10^4 \mu\text{m}$. Interestingly, Fig. 2A of [40] shows that *E. coli* cells can detect exponential up ramps with rate $r = 0.001/\text{s}$;

using $r = v_r/x_0$ where $v_r \approx 10\mu\text{m/s}$ is the *E. coli* run speed [38], this means that these cells are indeed able to sense very shallow gradients with $x_0 \approx 10^4\mu\text{m}$. Importantly, the predictions of our theory, Fig. 4, concern the shallowest gradient that the system with the optimal integration time can resolve: for any other integration time, the shallowest gradient will be steeper. These observations indicate that the optimal integration time is not only sufficient to make navigation in shallow gradients possible, but also necessary: to enable the detection of shallow gradients with $x_0 \approx 10^4\mu\text{m}$, as observed experimentally [40], the integration time *must* have been optimized. This is a strong prediction, since it implies that evolution has pushed the system to its sensing limits to enable navigation in shallow gradients.

Fig. 4 also shows that τ_r^{opt} decreases as the number of receptor-CheA complex, R_T , increases. As discussed in section III A, this is because a larger number of receptors allows for more instantaneous measurements, reducing the need for time integration. Interestingly, the data of Li and Hazelbauer [33] shows that the copy numbers of the chemotaxis proteins vary with the growth rate. Unfortunately, however, the response time has not been measured as a function of the growth rate. Clearly, it would be of interest to directly measure the response time in different strains under different growth conditions.

VI. DISCUSSION

Here, we have integrated ideas from Refs. [28–30] on information transmission via time-varying signals with the sampling framework of Ref. [12] to develop a unified theory of cellular sensing. The theory is founded on the concept of the dynamic input-output relation $p_{\tau_r}(L)$. It allows us to develop the idea that the cell employs the readout system to estimate the average receptor occupancy p_{τ_r} over the past integration time τ_r and then exploits the mapping $p_{\tau_r}(L)$ to estimate the current ligand concentration L from p_{τ_r} . The error in the estimate of L is then determined by how accurately the cell samples the receptor state to estimate p_{τ_r} , and by how much the ligand concentration in the past τ_r , which determines p_{τ_r} , reflects the current ligand concentration. These two distinct sources of error give rise to the sampling error and the dynamical error in Eq. 20, respectively.

While the system contains no less than 11 parameters, Eq. 20 provides an intuitive expression for the sensing error in terms of collective variables that have a clear interpretation. The dynamical error is only determined by the input noise strength σ_L/\bar{L} and the timescales in the problem—the correlation time τ_L of the input signal, the receptor correlation time τ_c , and the receptor integration time τ_r . The sampling error depends on the number of receptor samples, their independence, and their accuracy—these determine how accurately the receptor occupancy p is estimated—and on the timescales τ_r, τ_c, τ_L via the dynamical gain—this determines how the error in p propa-

gates to the estimate of the concentration. Eq. 20 shows that even when an infinite amount of cellular resources is devoted to sensing, reducing the sampling error to zero, the sensing error is still limited by the dynamical error when the integration time τ_r is finite. The dynamical error is a systematic error, which can only be eliminated by reducing τ_r to zero. However, while this increases the dynamic gain (which helps to reduce the sampling error), decreasing τ_r ultimately raises the sampling error, because the maximum number of independent concentration measurements per receptor is bounded by τ_r . Eq. 20 thus predicts that there exists an optimal integration time that optimizes the trade-off between minimizing the sampling error and the dynamical error.

Our study reveals that the optimal integration time τ_r^{opt} depends in a non-trivial manner on the design of the system. When the number of readout molecules X_T is smaller than the number of receptors R_T , time integration is not possible and the optimal system is an instantaneous responder with $\tau_r^{\text{opt}} = 0$. When the power $\dot{w} \sim X_T/\tau_r$, rather than X_T , is limiting, τ_r^{opt} is determined by the trade-off between the sampling error, set by X_T , and by the dynamical error, set by τ_r . In both scenarios, however, one resource, X_T or \dot{w} , is limiting the sensing precision. The other resources do not contribute to reducing the sensing error and are thus in excess, making these systems suboptimal.

In an optimally designed system all resources are equally limiting so that no resource is wasted. This yields the resource allocation principle, Eq. 31, first identified in Ref. [12]. That this design principle can be generalized to time-varying signals is not obvious because the sensing limits associated with the fundamental resources R_T , X_T , and \dot{w} , are different, corresponding to different sensing strategies with different τ_r^{opt} . However, our theory explains why Eq. 31 nonetheless still holds. The dynamics of the input signal affects both the dynamical error and the sampling error (see Eq. 20), but it influences the latter only via the dynamic gain, which influences how the error in the estimate of p_{τ_r} propagates to that in L . The input dynamics does not affect the error $\sigma_{p_{\tau_r}|L}^{2,\text{samp}}$ in estimating p_{τ_r} itself. Conversely, while $\sigma_{p_{\tau_r}|L}^{2,\text{samp}}$ depends on R_T , X_T and \dot{w} since they determine how accurately the receptor is sampled, the dynamical error and the dynamic gain do not depend on these resources but only on timescales. It is this non-trivial decomposition of the sensing error, which explains why the sensing limits set by the respective resources for a given τ_r (Eqs. 24, 26 and 28) have the same functional form, and why the allocation principle can be generalized. The design principle concerns the optimal allocation of resources for estimating p_{τ_r} , and this holds for any type of input signal: the number of independent concentration measurements at the receptor level is $R_T\tau_r/\tau_c$, irrespective of how the input varies, and in an optimally designed system this also equals the number of readout molecules X_T and energy $\beta\dot{w}\tau_r$ to store these measurements reliably.

While the allocation principle Eq. 31 holds for any τ_r ,

it does not specify the optimal integration time. However, our theory predicts that if the number of receptors is limiting, then there exists an optimal integration time τ_r^{opt} that maximizes the sensing precision for that number of receptors R_T (Eq. 24). Via the allocation principle Eq. 32, R_T and τ_r^{opt} then together determine the minimal number of readout molecules X_T and power \dot{w} to reach that precision. The resource allocation principle together with the optimal integration time thus completely specify the optimal design of the sensing system for a given number of receptors.

Our theory, via Eqs. 24 and 32, illuminates how the optimal design of a cellular sensing system depends on the dynamics of the input signal. In an optimal system, each receptor is sampled once every receptor-ligand correlation time τ_c , $\Delta \approx \tau_c$, and the number of samples per receptor is $\tau_r^{\text{opt}}/\Delta \approx \tau_r^{\text{opt}}/\tau_c$; the optimal integration time τ_r^{opt} is determined by the trade-off between the age of the samples and the number required for averaging the receptor state. When the input signal varies more rapidly and τ_L decreases, the samples need to be refreshed more regularly; to keep the dynamical error and the dynamic gain constant, τ_r^{opt} must decrease linearly with τ_L , see Eq. 20. Yet, only decreasing τ_r^{opt} would inevitably increase the sampling error $\sigma_{\hat{p}_{\tau_r|L}}^{2,\text{samp}}$ in estimating the receptor occupancy, because the sampling interval $\Delta \sim R_T \tau_r^{\text{opt}}/X_T^{\text{opt}}$ would become smaller than τ_c , causing the samples to contain redundant information. To keep the sensing precision constant, the number of receptors R_T needs to be raised with τ_L^{-1} , such that the sampling interval $\Delta \sim R_T \tau_r^{\text{opt}}/X_T^{\text{opt}}$ is again of order τ_c , and the decrease in the number of samples per receptor, $\tau_r^{\text{opt}}/\tau_c$, is precisely compensated for by the increase in R_T . The total number of independent concentration measurements, $R_T \tau_r^{\text{opt}}/\tau_c$, and hence the number of readout molecules X_T^{opt} to store these measurements, does indeed not change. In contrast, the required power $\dot{w}^{\text{opt}} = \dot{n} \Delta \mu \sim X_T^{\text{opt}} \Delta \mu / \tau_r^{\text{opt}}$ does increase: the readout molecules sample the receptor at a higher rate $\dot{n} \sim X_T^{\text{opt}} / \tau_r^{\text{opt}}$. Our theory thus predicts that when the input varies more rapidly, the number of receptors and the power must rise to maintain a required sensing precision, while the number of readout molecules does not.

While our theory makes concrete predictions on the optimal ratios of R_T , X_T , \dot{w} and τ_r given the statistics of the input signal, it does not predict what the optimal sensing precision and hence the absolute magnitudes of these resources are. In principle the cell can reduce the sensing error arbitrarily by increasing R_T and decreasing τ_r . Yet, the resource allocation principle, Eq. 32, shows that then not only the number of readout molecules needs to be raised, but also the power. Clearly, improving the sensing precision comes at a cost: more copies of the components of the sensing system need to be synthesized every cell cycle, and more energy is needed to run the system. The optimal sensing precision is determined by the trade-off between the fitness benefit of sensing and the energetic cost of maintaining and running the sens-

ing system, which is beyond the scope of our theory. We emphasize, however, that the resource allocation principle, Eq. 32, by itself is independent of the cost of the respective resources [12]: resources that are in excess cannot improve sensing and are thus wasted, no matter how cheap they are. It probably explains why our theory, without any fit parameters, not only predicts the integration time that allows *E. coli* to sense shallow gradients (Fig. 4), but also the number of receptor and readout molecules [12].

In our study we have limited ourselves to a canonical push-pull motif. However, the work of Ref. [12] indicates that our results hold more generally, pertaining also to sensing systems that employ cooperativity, negative or positive feedback, or consist of multiple layers, as the MAPK cascade. While multiple layers and feedback change the response time, they do not make time integration more efficient in terms of readout molecules or energy [12]. And provided it does not increase the correlation time of the signal [17, 42], cooperative ligand binding can reduce the sensing error per sample, but the resource requirements in terms of readout molecules and energy per sample do not change [12]. In all these systems, time integration requires that the history of the receptor is stored, which demands protein copies and energy.

Our performance measure—the precision by which the system can estimate the current concentration—is similar to that used to quantify the accuracy of measuring static concentrations [1, 4–9, 11, 12, 14]. This is the natural measure if one is interested in the question how accurately a cell can respond to the current concentration. Another performance measure is the learning rate or information flow, which quantifies the rate at which the system acquires information about the concentration [43–46]. An interesting question for future work would be whether systems that optimize the learning rate obey a resource allocation principle.

Lastly, in this paper we have studied the resource requirements for estimating the current concentration via the mechanism of time integration. However, to understand how *E. coli* navigates in a concentration gradient, we do not only have to understand how the system filters the high-frequency ligand-binding noise via time averaging, but also how on longer timescales the system adapts to changes in the ligand concentration [21]. This adaptation system also exhibits a trade-off between accuracy, speed and power [47, 48]. Intriguingly, simulations indicate that the combination of sensing (time integration) and adaptation allows *E. coli* not only to accurately estimate the current ligand concentration, but also predict the future ligand concentration [18]. It will be interesting to see whether an optimal resource allocation principle can be formulated for systems that need to predict future ligand concentrations.

ACKNOWLEDGMENTS

We wish to acknowledge Bela Mulder, Tom Shimizu and Tom Ouldrige for many fruitful discussions and a careful reading of the manuscript. This work is part of the research programme of the Netherlands Organisation for Scientific Research (NWO) and was performed at the research institute AMOLF.

SUPPORTING INFORMATION

Overview In this Supporting Information we derive the signal-to-noise ratio within the sampling framework, Eq. 20 of the main text, which is the principal result of our work. In this framework, the cell discretely samples the receptor state to estimate the average occupancy p_{τ_r} over the past integration time, and then inverts the dynamical input-output relation $p_{\tau_r}(L)$ to obtain the estimate for the current concentration $L(t)$.

First, however, we review the system and discuss the chemical Langevin equations that describe it. Then, in section S-II, we derive the expression for the sensing error based on estimating the concentration from the number of readout molecules x^* , Eq. S21. This is Eq. 4 of the main text.

In section S-III we derive the principal result of our work, the sensing error within the sampling framework, Eq. 20 of the main text. In S-IV we show that this result, for estimating the concentration from the time-averaged receptor occupancy, is the same as Eq. 4 and Eq. S21, for estimating the concentration from x^* .

In the next section, section S-V, we show how Eq. 20 of the main text can be rewritten as Eq. 23 of the main text. In section S-VI we discuss the optimal integration time while in S-VII we provide background information on the optimal resource allocation principle, Eq. 32 of the main text.

S-I. THE SYSTEM

The signal has a variance σ_L^2 and is assumed to relax exponentially with a correlation time $\tau_L = \lambda^{-1}$, as characterized by the correlation function $\langle \delta L(t) \delta L(t') \rangle = \sigma_L^2 e^{-\lambda(t-t')}$. The ligand can stochastically bind the receptor, while the ligand-bound receptor drives a push-pull network. In particular, the ligand-receptor complex catalyzes the phosphorylation of the readout molecules, while activated readouts can spontaneously decay, see Fig. 1 in the main text. This system is described by the following chemical reactions,



where L represents the free ligand, R the free receptor, RL the ligand-bound receptor, x^* the activated readout and x the deactivated readout. We also assume that the concentrations of ATP, ADP, and Pi are constant and absorbed in the rate constants. The cell needs to detect the total concentration $L(t) \equiv [L]_T(t)$ of ligand molecules, including both free and receptor-bound molecules, $[L]_T(t) = [L](t) + [RL](t)$. Moreover, since the total number of receptors R_T is constant, we can express the number of free receptors as $R(t) = R_T - RL(t)$. Similarly, the number of unphosphorylated readout molecules is $x(t) = X_T - x^*(t)$, with X_T the total number of readout molecules and x^* the number that is phosphorylated. Finally, we assume that we can neglect the sequestration of ligand molecules by the receptors, yielding $[L](t) \simeq [L]_T(t) = L(t)$ (for ease of notation we thus drop the subscript T on the total ligand concentration $L(t)$).

The chemical Langevin equations for this system read

$$\dot{RL}(t) = k_1 L(t)(R_T - RL(t)) - k_2 RL(t) + \eta_{RL} \quad (S4)$$

$$\dot{x}^*(t) = k_f RL(t)(X_T - x^*(t)) - k_{-f} RL(t)x^*(t) + k_{-r}(X_T - x^*(t)) - k_r x^*(t) + \eta_{x^*} \quad (S5)$$

with independent Gaussian white noise functions [49–53]. These equations reduce to the chemical rate equations for large copy numbers. We then apply the Linear-Noise Approximation (LNA) [54]: we expand the rate equations to first order around the steady-state of the mean-field chemical rate equations and compute the noise strength at this steady state. Comparison with computer simulations has revealed that when the system fluctuates in one basin of attraction, this description is surprisingly accurate even when the average copy numbers are as small as 10 molecules [52, 55]. In this approximation, the distribution of copy numbers is given by a multivariate Gaussian distribution [54]. It implies that the problem of computing the signal-to-noise ratio in Eq. 20 of the main text and thus the mutual information between the instantaneous values of the input and output reduces to calculating the variances and covariances of the corresponding copy numbers [20, 28]. We also emphasize that the external quantity $L(t)$ is a concentration, while the internal quantities R, RL, x, x^* are copy numbers.

We apply the LNA, expanding the ligand concentration and the receptor and readout copy numbers around their steady-state values as given by the mean-field chemical rate equations: $L(t) = \bar{L} + \delta L(t)$, $RL(t) = \bar{RL} + \delta RL(t)$ and $x^*(t) = \bar{x}^* + \delta x^*(t)$, with mean values $\bar{RL} = k_1 \bar{L} R_T / (k_2 + k_1 \bar{L}_T)$ and $\bar{x}^* = (k_f \bar{RL} + k_{-r}) X_T / ((k_f + k_{-f}) \bar{RL} + k_r + k_{-r})$. We then consider the Langevin dynamics of the new variables $\delta L(t)$, $\delta RL(t)$ and $\delta x^*(t)$ that describe the fluctuations around the corresponding mean values,

$$\delta \dot{RL}(t) = \rho \delta L(t) - \mu \delta RL(t) + \eta_{RL} \quad (S6)$$

$$\delta \dot{x}^*(t) = \rho' \delta RL(t) - \mu' \delta x^*(t) + \eta_{x^*}. \quad (S7)$$

In the first equation, $\mu = k_1 \bar{L} + k_2 = \tau_c^{-1}$ is the inverse of the receptor correlation time τ_c , $\rho = R_T k_1 (1 - p) =$

$p(1-p)R_{\text{T}}\mu/\bar{L}$, where $p = \bar{RL}/R_{\text{T}} = k_1\bar{L}/(k_2 + k_1\bar{L}) = k_1\bar{L}/\mu$ is the fraction of ligand-bound receptors. The second term on the r.h.s. represents the fluctuations in the ligand receptor binding at constant ligand concentration, while the first term arises from the fluctuations in the total ligand concentration. In the second equation, $\rho' = k_{\text{f}}X_{\text{T}}(1-f) - k_{\text{-f}}X_{\text{T}}f$ and $\mu' = (k_{\text{f}} + k_{\text{-f}})pR_{\text{T}} + k_{\text{r}} + k_{\text{-r}} = \tau_{\text{r}}^{-1}$ is the inverse of the integration time τ_{r} , where $f = \bar{x}^*/X_{\text{T}} = (k_{\text{f}}pR_{\text{T}} + k_{\text{-r}})/(k_{\text{f}} + k_{\text{-f}})pR_{\text{T}} + k_{\text{r}} + k_{\text{-r}} = (k_{\text{f}}pR_{\text{T}} + k_{\text{-r}})\tau_{\text{r}}$ is the fraction of phosphorylated readout molecules. The second term on the r.h.s. of Eq. S7 represents the fluctuations in the phosphorylation reaction at constant number of ligand-bound receptors, while the first term is due to fluctuations in the number of ligand-bound receptors.

The noise functions are given by [51]

$$\langle \eta_{RL}^2 \rangle = 2\mu R_{\text{T}} p(1-p) \quad (\text{S8})$$

$$\langle \eta_{x^*}^2 \rangle = 2\mu' X_{\text{T}} f(1-f) \quad (\text{S9})$$

where the cross-correlations $\langle \eta_L \eta_{RL} \rangle = \langle \eta_{x^*} \eta_L \rangle = \langle \eta_{x^*} \eta_{RL} \rangle = 0$ are zero because receptor-ligand binding does not affect the total ligand concentration and the complex RL acts as a catalyst in the push-pull network [52].

S-II. ESTIMATING THE CONCENTRATION FROM THE NUMBER OF READOUT MOLECULES x^*

Dynamic input-output relation The cell infers the current ligand concentration $L(t)$ from the instantaneous concentration of the output $x^*(t)$ and by inverting the input-output relation $\bar{x}^*(L)$. Since the ligand concentration fluctuates in time, and because the system will, in general, not respond instantly to these fluctuations, the input-output relation that the system must employ is the *dynamic* input-output relation, which yields the average readout concentration $\bar{x}^*(L)$ *given that* the current value of the time-varying signal is $L(t)$; here, the average is not only over the noise sources in the propagation of the signal from the input L to the output x^* —the receptor-ligand binding noise and the readout-phosphorylation noise (see Fig. 2(b) main text)—but also over the ensemble of input trajectories that each have the same current concentration $L(t)$ (see Fig. 2(c) main text) [28–30]. This dynamic input-output relation differs from the static input-output relation $\bar{x}^*(L_{\text{s}})$, which gives the average output concentration \bar{x}^* for a steady-state ligand concentration L_{s} that does not vary in time (or on a timescale that is much longer than that of the response). The slope of the dynamic input-output relation, which is key to the sensing precision, can be obtained from the Gaussian model discussed below.

Sensing error Linearizing $\bar{x}^*(L)$ around the mean concentration \bar{L} and using the rules of error propagation, the expected error in the concentration estimate is

then

$$(\delta\hat{L})^2 = \frac{\sigma_{x^*|L}^2}{\tilde{g}_{L \rightarrow x^*}^2}. \quad (\text{S10})$$

In this expression, $\sigma_{x^*|L}^2$ quantifies the width of the distribution of the output x^* *given* a value of the input signal L , while $\tilde{g}_{L \rightarrow x^*}$ is the dynamic gain, i.e. the slope of $\bar{x}^*(L)$ at \bar{L} .

Gaussian statistics We can obtain the variance $\sigma_{x^*|L}^2$ and the dynamic gain $\tilde{g}_{L \rightarrow x^*}$ within the Gaussian framework of the linear-noise approximation [28]. In the Gaussian model, the distribution of input values $L(t)$ and output values $x^*(t)$ is Gaussian around their mean values, \bar{L} and \bar{x}^* , respectively. We first define the deviations of L and x^* away from their mean values, respectively:

$$\delta L(t) = L(t) - \bar{L}, \quad (\text{S11})$$

$$\delta x^*(t) = x^*(t) - \bar{x}^*. \quad (\text{S12})$$

Since the dynamics of both L and x^* are stationary processes, we can choose to omit the explicit dependence on time, and simply write $\delta L(t) = \delta L$ and similarly for x^* . Defining the vector \mathbf{v} with components $\delta L(t), \delta x^*(t)$, the joint distribution can be written as

$$p(\mathbf{v}) = \frac{1}{\sqrt{2\pi^{2N}|\mathbf{Z}|}} \exp\left(-\frac{1}{2}\mathbf{v}^T \mathbf{Z}^{-1} \mathbf{v}\right) \quad (\text{S13})$$

where \mathbf{Z}^{-1} is the inverse of the matrix \mathbf{Z} , which has the following form:

$$\mathbf{Z} = \begin{pmatrix} \sigma_L^2 & \sigma_{L,x^*}^2 \\ \sigma_{L,x^*}^2 & \sigma_{x^*}^2 \end{pmatrix}. \quad (\text{S14})$$

From Eq. S13 it follows that the conditional distribution of δx^* given δL is

$$p(\delta x^* | \delta L) = \frac{1}{(2\pi\sigma_{x^*|L}^2)^{1/2}} \exp\left[-\frac{(\delta x^* - \bar{\delta x^*}(\delta L))^2}{2\sigma_{x^*|L}^2}\right]. \quad (\text{S15})$$

Dynamic gain In Eq. S15, $\bar{\delta x^*}(\delta L)$ is the average of the deviation $\delta x^*(\delta L) = x^*(\delta L) - \bar{x}^*$ of x^* from its mean \bar{x}^* given that the input is $\delta L = \delta L(t) = L(t) - \bar{L}$; it describes the dynamic input relation $\bar{x}^*(L)$ around $L = \bar{L}$. It is given by $\bar{\delta x^*}(\delta L) = \sigma_{L,x^*}^2 / \sigma_L^2 \delta L \equiv \tilde{g}_{L \rightarrow p\tau_{\text{r}}} \delta L$, which defines the dynamic gain:

$$\tilde{g}_{L \rightarrow p\tau_{\text{r}}} = \sigma_{L,x^*}^2 / \sigma_L^2. \quad (\text{S16})$$

Here, σ_L^2 is the variance of the input and σ_{L,x^*}^2 is the covariance between L and x^* , which is derived in Appendix S-A, see Eq. S97. It shows that the dynamic gain is

$$\tilde{g}_{L \rightarrow x^*} = \rho\rho' / ((\lambda + \mu)(\lambda + \mu')) = \tilde{g}_{L \rightarrow p\tau_{\text{r}}} \rho' R_{\text{T}} / \mu'. \quad (\text{S17})$$

In contrast to the macroscopic static gain $g_{L \rightarrow x^*} = dx^*/dL_s$, which characterizes the transmission of signals L_s that are constant in time, the dynamic gain depends both on parameters of the readout system and on the timescale of the input fluctuations τ_L . Only in the limit of slowly time-varying signals ($\tau_L \gg \tau_r, \tau_c$), does the dynamic gain $\tilde{g}_{L \rightarrow x^*}$ become equal to the static gain $g_{L \rightarrow x^*}$.

Conditional variance In Eq. S15, the variance $\sigma_{x^*|L}^2$ is the variance in x^* given that the signal is L . It is given by $\sigma_{x^*|L}^2 = |\mathbf{Z}|/\sigma_L^2$ [28], such that

$$\sigma_{x^*|L}^2 = \sigma_{x^*}^2 - \tilde{g}_{L \rightarrow p, \tau}^2 \sigma_L^2, \quad (\text{S18})$$

where $\sigma_{x^*}^2$ is the full variance of x^* , derived in Appendix S-A, see Eq. S94. Indeed, in this Gaussian model, the total variance $\sigma_{x^*}^2$ in the output x^* can be decomposed into a contribution from the variance $\tilde{g}_{L \rightarrow x^*}^2 \sigma_L^2$ due to variations in the signal itself, and a contribution from the variance $\sigma_{x^*|L}^2$ for a given value of the input L . The conditional variance $\sigma_{x^*|L}^2$ is shaped both by the noise in the propagation of the input L to the output x^* —stochastic receptor-ligand binding and noisy readout activation—and by the dynamics of the input signal.

Signal-to-noise ratio (SNR) The signal-to-noise ratio (SNR) is given by

$$\text{SNR} = \frac{\sigma_L^2}{(\delta \hat{L})^2}, \quad (\text{S19})$$

as discussed in the main text (see Eq. 3). Combining this expression with Eq. S10 yields the sensing error, the inverse SNR:

$$\text{SNR}^{-1} = \frac{\sigma_{x^*|L}^2}{\tilde{g}_{L \rightarrow x^*}^2 \sigma_L^2} = \frac{\sigma_L^2 \sigma_{x^*}^2}{\sigma_{L, x^*}^4} - 1, \quad (\text{S20})$$

where we have used Eqs. S16 and S18. Using the expressions for the variance for x^* , Eq. S94, and the covariance between L and x^* , Eq. S97, the signal-to-noise ratio reads

$$\begin{aligned} \text{SNR}^{-1} &= \frac{(\lambda + \mu)^2 (\lambda + \mu')^2}{\rho^2 \rho'^2 \sigma_L^2} f(1-f) X_T \\ &+ \frac{(\lambda + \mu)^2 (\lambda + \mu')^2}{\sigma_L^2 \mu' (\mu + \mu') \rho^2} p(1-p) R_T \\ &+ \frac{(\lambda + \mu)(\lambda + \mu')(\lambda + \mu + \mu')}{\mu \mu' (\mu + \mu')} - 1. \end{aligned} \quad (\text{S21})$$

This expression is difficult to interpret intuitively and impedes an analysis of the fundamental resources required for sensing. In contrast, the description of the readout system as a sampling device, presented in Sec. S-III, yields a much more illuminating expression for the sensing error, showing how it arises from a sampling error in estimating the receptor occupancy, set by the number of samples, their independence and their accuracy, and a dynamical error, set by the history of the input signal. In S-IV we show explicitly that these expressions are indeed identical.

Lastly, for the Gaussian model employed here, the SNR defined by Eq. S21, can be directly related to the mutual information [28, 56]:

$$I(L; x^*) = -\frac{1}{2} \ln(1 - r_{L, x^*}^2), \quad (\text{S22})$$

$$= \frac{1}{2} \ln(1 + \text{SNR}), \quad (\text{S23})$$

where $r_{L, x^*}^2 \equiv \sigma_{L, x^*}^4 / (\sigma_L^2 \sigma_{x^*}^2)$ is the correlation coefficient between input and output. This measure has also been used to quantify information transmission via time-varying signals [46, 57].

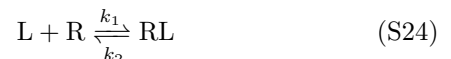
S-III. CALCULATING THE SNR WITHIN THE SAMPLING FRAMEWORK

In this section we derive the main result of our manuscript, namely the signal-to-noise ratio given by Eq. 20 of the main text. We derive this result by viewing the downstream network as a device that discretely samples the receptor state, first proposed in Ref. 12. The important quantities are the number of samples, the spacing between them, and the properties of the signal. The benefit of viewing the network as a sampling device is that the resulting expression has an intuitive interpretation: the more samples, the higher the signal-to-noise ratio; the further apart they are, the more independent they are. Moreover, in contrast to the static case, we see that even when the number of samples is very large, a systematic error remains when the integration time is finite; this dynamical error arises naturally within the sampling framework.

We first derive the signal-to-noise ratio for the irreversible push-pull network in section S-III A, and then generalize its expression to that of the full system in section S-III B. To help the reader in getting an overview of the derivation, we introduce several brief **overview paragraphs highlighted in bold, which elucidate the structure of the derivation.**

A. The SNR for the irreversible system derived within the sampling framework

We present the derivation of the signal-to-noise ratio within the sampling framework for the irreversible system, described by the following reactions:



The input signal $L(t)$ is modeled as a stationary signal with mean \bar{L} , variance σ_L^2 , and correlation time $\tau_L = \lambda^{-1}$. The relaxation of the deviation $\delta L(t) = L(t) - \bar{L}$ from

the mean signal \bar{L} is thus characterized by the correlation function $\langle \delta L(t) \delta L(t') \rangle = \sigma_L^2 e^{-\lambda(t-t')}$. The ligand molecules bind the receptor molecules stochastically with receptor correlation time $\tau_c = k_1 \bar{L}_T + k_2 = \mu^{-1}$. The readout molecules X interact with the receptor such that the ligand binding state of the receptor is copied into the chemical modification state of the readout. We consider the limit that the total number of readout molecules X_T is large, such that the fraction of phosphorylated readout molecules $f = k_f p R_T / (k_f p R_T + k_r)$ is small and $\bar{x} \simeq X_T$. The integration time of this system is $\tau_r = (k_f p R_T + k_r)^{-1} = \mu^{-1}$.

We view the downstream readout system as a sampling device that estimates the average receptor occupancy over the integration time τ_r from the active readout molecules $x^*(L(t)) = x^*(L)$ via

$$\hat{p}_{\tau_r} = \frac{x^*(L)}{\bar{N}}, \quad (\text{S27})$$

where \bar{N} is the average of the number of samples N taken during the integration time τ_r .

The number of active readout molecule $x^*(t)$ at time t is given by

$$x^*(t) = \sum_{i=1}^N n_i(t_i), \quad (\text{S28})$$

where n_i is the state of the i th sample, corresponding to the state of the receptor involved in the i th collision at time $t_i < t$: $n_i(t_i) = 1$ if receptor is ligand bound and $n_i(t_i) = 0$ otherwise. The total rate at which inactive readout molecules interact with the receptor—the sampling rate—is given by $r = k_f \bar{x} R_T \approx k_f X_T R_T$ and the average number of samples obtained during the integration time τ_r is

$$\bar{N} = k_f X_T R_T \tau_r. \quad (\text{S29})$$

We also note here that the flux of readout molecules is $\dot{n} = r p$ and, using that $f = k_f p R_T \tau_r$, the average number of samples is also given by $\bar{N} = f(1-f) X_T / p \approx f X_T / p$.

The cell then estimates the concentration via its estimate of the receptor occupancy \hat{p}_{τ_r} and by inverting the dynamic input-output relation $p_{\tau_r}(L)$. Via error propagation this yields the error

$$(\delta \hat{L})^2 = \frac{\sigma_{\hat{p}_{\tau_r}|L}^2}{\tilde{g}_{L \rightarrow p_{\tau_r}}^2}, \quad (\text{S30})$$

where $\sigma_{\hat{p}_{\tau_r}|L}^2$ is the variance in the estimate of p_{τ_r} given the ligand concentration $L(t)$, and $\tilde{g}_{L \rightarrow p_{\tau_r}}$ is the dynamic gain $\tilde{g}_{L \rightarrow p_{\tau_r}} \equiv dp_{\tau_r}(L)/dL$. Defining the signal-to-noise ratio as $\text{SNR} = \sigma_L^2 / (\delta \hat{L})^2$, where σ_L^2 is the variance of the ligand concentration, this yields

$$\text{SNR}^{-1} = \frac{(\delta \hat{L})^2}{\sigma_L^2} = \frac{\sigma_{\hat{p}_{\tau_r}|L}^2}{\tilde{g}_{L \rightarrow p_{\tau_r}}^2 \sigma_L^2}. \quad (\text{S31})$$

Overview We first derive the dynamic gain and then in the section **Error in estimating receptor occupancy** the error $\sigma_{\hat{p}_{\tau_r}|L}^2$.

Dynamic gain The dynamic gain quantifies how much a ligand fluctuation at time t , $\delta L(t)$, leads to a change δp_{τ_r} in the average receptor occupancy $p_{\tau_r} = \langle n(t) \rangle_{\tau_r}$ over the past integration time τ_r . The average of the receptor occupancy is taken by the readout molecules downstream of the receptor: these molecules at time t provide the samples of the state of the receptor at the earlier times t_i . As shown in Ref. 12, the probability that a readout molecule at time t provides a sample of the receptor at an earlier time t_i is $p(t_i|\text{sample}) = e^{-(t-t_i)/\tau_r} / \tau_r$. Hence, the average change in the receptor occupancy over the past integration time τ_r is

$$\delta p_{\tau_r} = E \langle \delta n(t_i) \rangle_{\delta L(t)} \quad (\text{S32})$$

$$= \int_{-\infty}^t dt_i \langle \delta n(t_i) \rangle_{\delta L(t)} \frac{e^{-(t-t_i)/\tau_r}}{\tau_r}. \quad (\text{S33})$$

Here, E denotes the expectation over the sampling times t_i , $\langle \delta n(t_i) \rangle_{\delta L(t)}$ is the average deviation in the receptor occupancy at time t_i , $\langle \delta n(t_i) \rangle_{\delta L(t)} \equiv \langle n(t_i) \rangle_{\delta L(t)} - p$, given that the ligand concentration at time t is $\delta L(t)$; this average is taken over receptor-ligand binding noise and the subensemble of trajectories ending at $\delta L(t)$, see Fig. 2(c) of the main text. We can compute it within the linear-noise approximation:

$$\langle \delta n(t_i) \rangle_{\delta L(t)} = \rho_n \int_{-\infty}^{t_i} dt' \langle \delta L(t') \rangle_{\delta L(t)} e^{-(t_i-t')/\tau_c}, \quad (\text{S34})$$

where $\rho_n = p(1-p)/(\bar{L}_T \tau_c)$ and $\langle \delta L(t') \rangle_{\delta L(t)}$ is the average ligand concentration at time t' given that the ligand concentration at time t is $\delta L(t)$. It is given by [30]

$$\langle \delta L(t') \rangle_{\delta L(t)} = \delta L(t) e^{-|t-t'|/\tau_L}. \quad (\text{S35})$$

Combining Eqs. S33-S35 yields the following expression for the average change in the average receptor occupancy p_{τ_r} , given that the ligand at time t is $\delta L(t)$:

$$\langle \delta n(t) \rangle_{\delta L(t)}^{\tau_r} = \frac{p(1-p)}{\bar{L}_T} \left(1 + \frac{\tau_c}{\tau_L}\right)^{-1} \left(1 + \frac{\tau_r}{\tau_L}\right)^{-1} \delta L(t), \quad (\text{S36})$$

$$= \tilde{g}_{L \rightarrow p_{\tau_r}} \delta L(t). \quad (\text{S37})$$

Hence the dynamic gain is

$$\tilde{g}_{L \rightarrow p_{\tau_r}} = \frac{p(1-p)}{\bar{L}} \left(1 + \frac{\tau_c}{\tau_L}\right)^{-1} \left(1 + \frac{\tau_r}{\tau_L}\right)^{-1}, \quad (\text{S38})$$

$$= g_{L \rightarrow p} \left(1 + \frac{\tau_c}{\tau_L}\right)^{-1} \left(1 + \frac{\tau_r}{\tau_L}\right)^{-1}. \quad (\text{S39})$$

The dynamic gain is the average change in the receptor occupancy p_{τ_r} over the past integration time τ_r given that

the change in the ligand concentration at time t is $\delta L(t)$. It depends on all the timescales in the problem, and only reduces to the static gain $g_{L \rightarrow p} = p(1-p)/\bar{L}$ when the integration time τ_r and the receptor correlation time τ_c are both much shorter than the ligand correlation time τ_L . The dynamic gain determines how much an error in the estimate of p_{τ_r} propagates to the estimate of $L(t)$.

Error in estimating receptor occupancy Using the law of total variance, the error $\sigma_{\hat{p}_{\tau_r}|L}^2$ in the estimate of the receptor occupancy p_{τ_r} over the past integration time τ_r is given by

$$\sigma_{\hat{p}_{\tau_r}|L}^2 = \text{var} [E(\hat{p}_{\tau_r}|L|N)] + E [\text{var}(\hat{p}_{\tau_r}|L|N)]. \quad (\text{S40})$$

The first term reflects the variance of the mean of $\hat{p}_{\tau_r}|L$ given the number of samples N ; the second term reflects the mean of the variance in $\hat{p}_{\tau_r}|L$ given the number of samples N [12].

Overview We first discuss the first term and then the second term on the right-hand side of Eq. S40. The second term contains two contributions; one combines with the first term to give rise to the sampling error, while the other yields the dynamical error of Eq. 20 of the main text.

Error from stochasticity in number of samples The first term of Eq. S40 describes the noise that arises from the stochasticity in the number of samples. It can be written as

$$\text{var} [E(\hat{p}_{\tau_r}|L|N)] = \text{var} \left[\frac{1}{N} E \left(\sum_{i=1}^N n(t_i) \middle| N \right) \right] \quad (\text{S41})$$

where we have dropped the subscript i on n_i (compare against Eq. S28) because in estimating the average receptor occupancy we can focus on a single receptor. The above average can be written as

$$E \left(\sum_{i=1}^N n(t_i) \middle| N \right) = N \overline{E \langle n(t_i) \rangle_{\delta L(t)}}, \quad (\text{S42})$$

$$= N \left(p + \overline{E \langle \delta n(t_i) \rangle_{\delta L(t)}} \right), \quad (\text{S43})$$

$$= N \left(p + \overline{\tilde{g} \delta L(t)} \right), \quad (\text{S44})$$

$$= Np. \quad (\text{S45})$$

Here the angular brackets $\langle \dots \rangle_{\delta L(t)}$ denote an average over the ligand binding state of the receptor, with the subscript $\delta L(t)$ indicating that the average is to be taken for a given $\delta L(t)$. The expectation E denotes an average over all samples times t_i (see also Eq. S32), and the overline indicates an average over $\delta L(t)$. In going from the second to the third line we have used Eq. S37, with \tilde{g} the short-hand notation for $\tilde{g} = \tilde{g}_{L \rightarrow p_{\tau_r}}$, as also used

below unless stated otherwise. Hence, Eq. S41 becomes

$$\text{var} [E(\hat{p}_{\tau_r}|L|N)] = \text{var} \left[\frac{N}{N} p \right], \quad (\text{S46})$$

$$= \frac{p^2}{N^2} \text{var} [N], \quad (\text{S47})$$

$$= \frac{p^2}{N}. \quad (\text{S48})$$

This term is governed by the nature of the sampling process and does not depend on the statistics of the input signal. It is indeed the same as that for sensing static concentrations [12].

Error for fixed number of samples The second term of Eq. S40 describes the error in the estimate of $p_{\tau_r}|L$ that arises for a fixed number of samples. It is given by

$$E [\text{var}(\hat{p}_{\tau_r}|L|N)] = E \left[\frac{N^2}{N^2} \text{var} \left(\frac{\sum_{i=1}^N n_i(t_i)}{N} \middle| N \right) \right] \quad (\text{S49})$$

In Appendix S-B we show that

$$\begin{aligned} & \text{var} \left(\frac{\sum_{i=1}^N n_i(t_i)}{N} \middle| N \right) \\ &= \frac{p(1-p)}{N} + \overline{E \langle \delta n_i(t_i) \delta n_j(t_j) \rangle_{\delta L(t)}} - \tilde{g}^2 \sigma_L^2, \end{aligned} \quad (\text{S50})$$

where $\delta n_i(t_i) = n_i(t_i) - p$ and E denotes an average over the sampling times t_i . As we show next, the receptor covariance $\overline{E \langle \delta n_i(t_i) \delta n_j(t_j) \rangle_{\delta L(t)}}$ splits into two contributions, one that together with the first term of Eq. S50 and with Eq. S48 forms the sampling error, and one that together with the last term of Eq. S50, $-\tilde{g}^2 \sigma_L^2$, forms the dynamical error of Eq. 20 of the main text.

The receptor covariance To derive the receptor covariance $\overline{E \langle \delta n_i(t_i) \delta n_j(t_j) \rangle_{\delta L(t)}}$, the second term of Eq. S50, we note that the deviation $\delta n_i(t_i) = n_i(t_i) - p$ of the receptor occupancy $n_i(t_i)$ from the mean p is

$$\delta n_i(t_i) = \int_{-\infty}^{t_i} dt' e^{-(t_i-t')/\tau_c} [\rho_n \delta L(t') + \xi_i(t')], \quad (\text{S51})$$

where $\xi_i(t')$ models the ligand-binding noise of the receptor i at time t' . The covariance for a given $\delta L(t)$ is then given by the sum of two contributions,

$$\begin{aligned} & \langle \delta n_i(t_i) \delta n_j(t_j) \rangle_{\delta L(t)} = \\ & \underbrace{\rho_n^2 \int_{-\infty}^{t_i} dt' \int_{-\infty}^{t_j} dt'' e^{-(t_i-t')/\tau_c} \langle \delta L(t') \delta L(t'') \rangle_{\delta L(t)} e^{-(t_j-t'')/\tau_c}}_{\text{covS}} \\ & + \underbrace{\int_{-\infty}^{t_i} dt' \int_{-\infty}^{t_j} dt'' e^{-(t_i-t')/\tau_c} \langle \xi_i(t') \xi_j(t'') \rangle e^{-(t_j-t'')/\tau_c}}_{\text{covR}}. \end{aligned} \quad (\text{S52})$$

Hence, the receptor covariance averaged over $\delta L(t)$ and the sampling times is

$$\begin{aligned} \overline{E[\langle \delta n_i(t_i) \delta n_j(t_j) \rangle_{\delta L(t)}]} &= \overline{E[\text{covS}(n_i(t_i), n_j(t_j))]} \\ &+ \overline{E[\text{covR}(n_i(t_i), n_j(t_j))]} . \end{aligned} \quad (\text{S53})$$

Overview The first term on the right-hand side of Eq. S53 describes the receptor covariance due to the ligand and concentration fluctuations. Together with the third term of Eq. S50, $-\tilde{g}^2 \sigma_L^2$, it forms the dynamical error in estimating p_{τ_r} (Eq. 18 main text). The second term of Eq. S53 characterizes the correlations in the receptor switching that arise from the stochastic ligand binding and unbinding. This term forms, together with Eq. S48 and with the first term of Eq. S50, the sampling error in estimating p_{τ_r} (Eq. 17 main text). We will now first show how these three terms yield the sampling error. We will then return to the first term on the right-hand side of Eq. S53 and show how that with $-\tilde{g}^2 \sigma_L^2$ it forms the dynamical error.

Receptor switching noise In Eq. S52, $\langle \xi_i(t') \xi_j(t'') \rangle = \langle \xi^2 \rangle \delta(t' - t'')$ where the noise amplitude $\langle \xi^2 \rangle = 2p(1-p)/(R_T \tau_c)$ is divided by R_T because we assume that the ligand molecules bind the receptors independently, thus ignoring spatio-temporal correlations [17]. The second term of Eq. S52 then yields

$$\text{covR}(n_i(t_i), n_j(t_j)) = \frac{p(1-p)}{R_T} e^{-|t_j - t_i|/\tau_c}. \quad (\text{S54})$$

We now perform the averaging over the sampling times, denoted by E . It is convenient to express and evaluate the integrals in terms of $\lambda = 1/\tau_L$, $\mu = 1/\tau_c$, and $\mu' = 1/\tau_r$. Using that the probability that a readout molecule at time t has taken a sample of the receptor at an earlier time t_i is $p(t_i | \text{sample}) = e^{-(t-t_i)/\tau_r}/\tau_r$ [12], we obtain

$$\begin{aligned} E[\text{covR}(n_i(t_i), n_j(t_j))] &= \frac{p(1-p)\mu'^2}{R_T} \int_{-\infty}^t dt_i \int_{-\infty}^t dt_j e^{-\mu'(t-t_i)} e^{-\mu'(t-t_j)} e^{-\lambda|t_j-t_i|} \\ & \quad (\text{S55}) \end{aligned}$$

$$= \frac{p(1-p)\mu'^2}{R_T} e^{-2\mu' t} \int_{-\infty}^t dt_j e^{2\mu' t_j} 2 \int_0^\infty d\tilde{\Delta} e^{-(\mu'+\mu)\tilde{\Delta}} \quad (\text{S56})$$

$$= \frac{p(1-p)}{R_T} \frac{\tau_c}{\tau_c + \tau_r} \simeq \frac{p(1-p)}{R_T} \frac{\tau_c}{\tau_r}, \quad (\text{S57})$$

where $\tilde{\Delta} = |t_j - t_i|$ and in the last line we have used that typically $\tau_r \gg \tau_c$. Clearly, the above expression is the same for each value of the signal $\delta L(t)$ and does not need to be averaged over $\delta L(t)$.

The sampling error Eq. S57 forms with the first term of Eq. S50 the sampling error for a fixed number of

samples N (see Ref. 12):

$$\text{var} \left(\frac{\sum_{i=1}^N n_i(t_i)}{N} \right)^{\text{samp}} = \frac{p(1-p)}{N} \left(1 + \frac{2N\tau_c}{2R_T\tau_r} \right), \quad (\text{S58})$$

$$= \frac{p(1-p)}{f_I N}, \quad (\text{S59})$$

where

$$f_I = \frac{1}{1 + 2\tau_c/\Delta} \quad (\text{S60})$$

is the fraction of independent samples with $\Delta = 2R_T\tau_r/N$ being the spacing between the receptor samples. We now have to average Eq. S59 over the different number of samples N (see Eq. S49), which finally gives

$$E[\text{var}(\hat{p}_{\tau_r|L}|N)]^{\text{samp}} = \frac{p(1-p)}{f_I \bar{N}}. \quad (\text{S61})$$

This equation has a very clear interpretation: it is the error in the estimate of the receptor occupancy based on a single measurement—given by the variance of the receptor occupancy $p(1-p)$ —divided by the total number of independent measurements $f_I \bar{N}$.

Eq. S48 and Eq. S61 together yield the sampling error in estimating the receptor occupancy

$$\sigma_{\hat{p}_{\tau_r|L}}^{2, \text{samp}} = \frac{p^2}{\bar{N}} + \frac{p(1-p)}{f_I \bar{N}}. \quad (\text{S62})$$

To know how the error $\sigma_{\hat{p}_{\tau_r|L}}^{2, \text{samp}}$ in the estimate of the receptor occupancy propagates to the error $(\delta \hat{L})^2$ in the estimate of the concentration (see Eq. S30), we need to divide this error by the dynamic gain, given by Eq. S38. Via Eq. S31 this then yields the inverse signal-to-noise ratio associated with the sampling error:

$$\begin{aligned} \text{SNR}_{\text{samp}}^{-1} &= \left(1 + \frac{\tau_c}{\tau_L} \right)^2 \left(1 + \frac{\tau_r}{\tau_L} \right)^2 \left[\frac{(\bar{L}/\sigma_L)^2}{p(1-p)f_I \bar{N}} + \frac{(\bar{L}/\sigma_L)^2}{(1-p)^2 \bar{N}} \right]. \\ & \quad (\text{S63}) \end{aligned}$$

Dynamical error In estimating a time-varying ligand and concentration, the sensing error arises not only from the stochastic sampling of the receptor state, but also from the fact that the current ligand concentration corresponds to an ensemble of ligand trajectories in the past, which each give rise to a different integrated receptor occupancy. This effect is contained in the first term of Eq. S53. Crucially, the averaging over $\delta L(t)$ can be performed before the averaging over the sampling times, such that $\overline{E[\text{covS}(n_i(t_i), n_j(t_j))]} = E[\text{covS}(n_i(t_i), n_j(t_j))]$ with

$$\begin{aligned} \overline{\text{covS}(n_i(t_i), n_j(t_j))} &= \\ \rho_n^2 \int_{-\infty}^{t_i} dt' \int_{-\infty}^{t_j} dt'' e^{-(t_i-t')/\tau_c} \overline{\langle \delta L(t') \delta L(t'') \rangle_{\delta L(t)}} e^{-(t_j-t'')/\tau_c}. \end{aligned} \quad (\text{S64})$$

We can now exploit that $\overline{\langle \delta L(t') \delta L(t'') \rangle_{\delta L(t)}} = \langle \delta L(t') \delta L(t'') \rangle = \sigma_L^2 e^{-\lambda|t''-t'|}$. Inserting this into Eq. S64 and integrating it yields

$$\overline{\text{covS}(n_i(t_i), n_j(t_j))} = \rho_n^2 \sigma_L^2 \frac{\lambda e^{-\mu(t_j-t_i)} - \mu e^{-\lambda(t_j-t_i)}}{\mu(\lambda^2 - \mu^2)}. \quad (\text{S65})$$

We now again average over the sample times

$$E[\overline{\text{covS}(n_i(t_i), n_j(t_j))}] \quad (\text{S66})$$

$$\mu'^2 \int_{-\infty}^t dt_i \int_{-\infty}^t dt_j e^{-\mu'(t-t_i)} \overline{\text{covS}(n_i(t_i), n_j(t_j))} e^{-\mu'(t-t_j)} \quad (\text{S67})$$

$$= \rho_n^2 \sigma_L^2 \frac{\mu'(\lambda + \mu + \mu')}{\mu(\mu + \lambda)(\mu + \mu')(\mu' + \lambda)} \quad (\text{S68})$$

$$= \frac{\rho_n^2 \mu'^2 \sigma_L^2}{(\mu + \lambda)^2 (\mu' + \lambda)^2} \frac{(\lambda + \mu + \mu')(\mu + \lambda)(\mu' + \lambda)}{\mu' \mu (\mu + \mu')} \quad (\text{S69})$$

$$= \tilde{g}^2 \sigma_L^2 \frac{(\lambda + \mu + \mu')(\mu + \lambda)(\mu' + \lambda)}{\mu' \mu (\mu + \mu')} \quad (\text{S70})$$

$$= \tilde{g}^2 \sigma_L^2 \left(1 + \frac{\tau_c}{\tau_L}\right) \left(1 + \frac{\tau_r}{\tau_L}\right) \left(1 + \frac{\tau_c \tau_r}{\tau_L(\tau_c + \tau_r)}\right). \quad (\text{S71})$$

Importantly, the above expression is not the dynamical error in the estimate of the receptor occupancy. It is the receptor covariance that arises from the signal fluctuations, but this contains a contribution from the dynamical error *and* the signal variations of interest, $\tilde{g}^2 \sigma_L^2$. To obtain the dynamical error in the receptor occupancy, we have to subtract from the above expression $\tilde{g}^2 \sigma_L^2$, which is indeed the third term of Eq. S50—the term that we had not yet taken care-off. This procedure directly yields the dynamical error in the receptor occupancy, because the above expression does not depend on the number of samples N , so there is no need to average over N in Eq. S49. We thus immediately find

$$\sigma_{\hat{p}_{\tau_r|L}}^2, \text{ dyn} = \tilde{g}^2 \sigma_L^2 \left[\left(1 + \frac{\tau_c}{\tau_L}\right) \left(1 + \frac{\tau_r}{\tau_L}\right) \left(1 + \frac{\tau_c \tau_r}{\tau_L(\tau_c + \tau_r)}\right) - 1 \right] \quad (\text{S72})$$

To obtain the contribution from the dynamical error to the signal-to-noise ratio we divide Eq. S72 by the dynamic gain and the signal variance, see Eq. S31. This yields

$$\text{SNR}_{\text{dyn}}^{-1} = \left(1 + \frac{\tau_c}{\tau_L}\right) \left(1 + \frac{\tau_r}{\tau_L}\right) \left(1 + \frac{\tau_c \tau_r}{\tau_L(\tau_c + \tau_r)}\right) - 1. \quad (\text{S73})$$

Interestingly, this contribution only depends on the timescales in the problem, which can be understood by noting it arises from the fact that the signal in the past deviates, in general, from the current signal. It thus neither depends on the number of receptors nor on the number of readout molecules that store the receptor state.

Sensing error Summing Eqs. S63 and S73 gives the sensing error for the irreversible system. In the next subsection, we show how the principal result of our study, Eq. 20, the sensing error for the full system, can be cast in precisely the same form.

Check We can check the final expression for the sensing error as derived within the sampling framework, by computing $\sigma_{x^*|L}^2$ in the linear-noise approximation and exploiting that $\hat{p}_{\tau_r} = x^*/\bar{N}$ (see Eq. S28) such that $\sigma_{\hat{p}_{\tau_r}|L}^2 = \sigma_{x^*|L}^2/\bar{N}^2$, with $\bar{N} = k_f X_T R_T \tau_r$. In section S-II we derived $\sigma_{x^*|L}^2$ and the gain $\tilde{g}_{L \rightarrow x^*}^2$ for the reversible system. Taking the irreversible limit, $k_{-f} \rightarrow 0$ and $k_{-r} \rightarrow 0$, then yields via $\text{SNR}^{-1} = \sigma_{x^*|L}^2/(\tilde{g}_{L \rightarrow x^*}^2 \sigma_L^2)$ indeed the same result for the sensing error.

B. The SNR for the general reversible system derived within the sampling framework

We can derive the principal result of the main text, Eq. 20, for the fully reversible system by exploiting the mapping

$$\sigma_{\hat{p}_{\tau_r|L}}^2 = \frac{\sigma_{x^*|L}^2}{\bar{N}^2}, \quad (\text{S74})$$

where $\sigma_{\hat{p}_{\tau_r|L}}^2$ is the variance in the estimate of the receptor occupancy over the integration time τ_r , and $\sigma_{x^*|L}^2$ is the variance in the number of phosphorylated readout molecules, both conditioned on the signal being $\delta L(t)$. The conditional variance (see Eq. S18)

$$\sigma_{x^*|L}^2 = \sigma_{x^*}^2 - \tilde{g}_{L \rightarrow x^*}^2 \sigma_L^2 \quad (\text{S75})$$

is the full variance $\sigma_{x^*}^2$ of x^* minus the variance $\tilde{g}_{L \rightarrow x^*}^2 \sigma_L^2$ that is due to the signal variations, given by the dynamic gain $\tilde{g}_{L \rightarrow x^*}^2$ from L to x^* times the signal variance σ_L^2 .

The full variance of the readout $\sigma_{x^*}^2$ in Eq. S75 is given by Eq. S94 of Appendix S-A, where we derive the variances and covariances of the ligand, receptor and the readout. In this expression, $\mu = \tau_c^{-1} = k_1 \bar{L} + k_2$ is the inverse of the receptor correlation time τ_c ; $p = \bar{R} \bar{L} / R_T = k_1 \bar{L} / (k_2 + k_1 \bar{L}) = k_1 \bar{L} \tau_c$ is the probability that a receptor is bound to ligand; $\rho = R_T k_1 (1 - p) = p(1 - p) R_T \mu / \bar{L}$; $\mu' = (k_f + k_{-f}) p R_T + k_r + k_{-r} = \tau_r^{-1}$ is the inverse of the integration time τ_r ; $f = \bar{x}^* / X_T = (k_f p R_T + k_{-r}) \tau_r$ is the fraction of phosphorylated readout; $\rho' = k_f X_T (1 - f) - k_{-f} X_T f = \dot{n} / (p R_T)$ is the sampling rate \dot{n} of the receptor, be it ligand bound or not. Moreover, the quality factor $q = (e^{\Delta \mu_1} - 1)(e^{\Delta \mu_2} - 1) / (e^{\Delta \mu} - 1) = \rho' p R_T \tau_r / (f(1 - f) X_T) = \dot{n} \tau_r / (f(1 - f) X_T)$ (see Appendix S-C).

To get $\sigma_{\hat{p}_{\tau_r|L}}^2$ from Eqs. S74 and S75 we need not only $\sigma_{x^*}^2$ (Eq. S94), but also the average number of samples \bar{N} and the dynamic gain $\tilde{g}_{L \rightarrow x^*}^2$. The average number of samples taken during the integration time τ_r is $\bar{N} = r \tau_r = \dot{n} \tau_r / p = f(1 - f) X_T q / p = \rho' R_T / \mu'$ and the

effective number of reliable samples is $\bar{N}_{\text{eff}} = q\bar{N}$. Moreover, Eq. S17 reveals that the dynamic gain from L to x^* is given by [28]

$$\tilde{g}_{L \rightarrow x^*} = \frac{\sigma_{L,x^*}^2}{\sigma_L^2} = \tilde{g}_{L \rightarrow p_{\tau_r}} R_T \frac{\rho'}{\mu'} = \tilde{g}_{L \rightarrow p_{\tau_r}} \bar{N}. \quad (\text{S76})$$

Hence, combining Eqs. S74-S76 with Eq. S94 yields

$$\begin{aligned} \sigma_{\hat{p}_{\tau_r|L}}^2 &= \frac{p^2}{\bar{N}_{\text{eff}}} + \frac{p(1-p)}{\bar{N}_{\text{eff}}} + \frac{p(1-p)}{R_T(1+\tau_r/\tau_c)} \\ &+ \tilde{g}_{L \rightarrow p_{\tau_r}}^2 \sigma_L^2 \left(1 + \frac{\tau_c}{\tau_L}\right) \left(1 + \frac{\tau_r}{\tau_L}\right) \left(1 + \frac{\tau_c \tau_r}{\tau_L(\tau_c + \tau_r)}\right) \\ &- \tilde{g}_{L \rightarrow p_{\tau_r}}^2 \sigma_L^2. \end{aligned} \quad (\text{S77})$$

This can be rewritten using the expression for the fraction of independent samples, which, assuming that $\tau_r \gg \tau_c$, is $f_I = 1/(1+2\tau_c/\Delta)$, with $\Delta = 2\tau_r R_T/\bar{N}_{\text{eff}}$ the effective spacing between the samples:

$$\begin{aligned} \sigma_{\hat{p}_{\tau_r|L}}^2 &= \frac{p^2}{\bar{N}_{\text{eff}}} + \frac{p(1-p)}{f_I \bar{N}_{\text{eff}}} \\ &+ \tilde{g}^2 \sigma_L^2 \left[\left(1 + \frac{\tau_c}{\tau_L}\right) \left(1 + \frac{\tau_r}{\tau_L}\right) \left(1 + \frac{\tau_c \tau_r}{\tau_L(\tau_c + \tau_r)}\right) - 1 \right]. \end{aligned} \quad (\text{S78})$$

Importantly, this expression has exactly the same form as that for the irreversible case (Sec. S-III A), obtained by combining Eqs. S62 and S72, but with \bar{N} replaced by $\bar{N}_{\text{eff}} = q\bar{N}$ and $\bar{N}_I = f_I \bar{N}$ by $f_I \bar{N}_{\text{eff}}$. This shows that also for the fully reversible case we can view the readout system as a device that discretely samples the receptor state to estimate the occupancy, from which the concentration is then inferred.

Combining Eq. S78 with Eqs. S31 and S38 finally yields the principal result of our work, Eq. 20 of the main text.

S-IV. ESTIMATING CONCENTRATION FROM x^* IS NO DIFFERENT FROM ESTIMATING IT FROM p_{τ_r} : REWRITING EQ. 4 OF MAIN TEXT INTO EQ. 20

Eq. 4 of the main text (Eq. S21 of *SI*) can be rewritten to yield exactly the same expression as Eq. 20 of the main text, as it must be possible. To show the equivalence, it is convenient to exploit that $\rho = p(1-p)R_T\mu/(\bar{L})$, $\bar{N} = \dot{n}\tau_r/p = (\rho'/\mu')R_T$, $q = \rho'pR_T\tau_r/(f(1-f)X_T)$ (see Appendix S-C) and to split the first term on the right-

hand side of Eq. S21:

$$\begin{aligned} \text{SNR}^{-1} &= \left(1 + \frac{\tau_c}{\tau_L}\right)^2 \left(1 + \frac{\tau_r}{\tau_L}\right)^2 \left[\frac{f(1-f)X_T\mu'^2(\bar{L}/\sigma_L)^2}{\rho'^2(p(1-p)R_T)^2} \right. \\ &+ \left. \frac{(\bar{L}/\sigma_L)^2}{p(1-p)R_T(1+\tau_r/\tau_c)} \right] \\ &+ \left(1 + \frac{\tau_c}{\tau_L}\right) \left(1 + \frac{\tau_r}{\tau_L}\right) \left(1 + \frac{\tau_c \tau_r}{\tau_L(\tau_c + \tau_r)}\right) - 1, \quad (\text{S79}) \\ &= \left(1 + \frac{\tau_c}{\tau_L}\right)^2 \left(1 + \frac{\tau_r}{\tau_L}\right)^2 \left[\frac{(\bar{L}/\sigma_L)^2}{\bar{N}_{\text{eff}}(1-p)^2} + \frac{(\bar{L}/\sigma_L)^2}{p(1-p)\bar{N}_{\text{eff}}} \right. \\ &+ \left. \frac{(\bar{L}/\sigma_L)^2}{p(1-p)R_T(1+\tau_r/\tau_c)} \right] \\ &+ \left(1 + \frac{\tau_c}{\tau_L}\right) \left(1 + \frac{\tau_r}{\tau_L}\right) \left(1 + \frac{\tau_c \tau_r}{\tau_L(\tau_c + \tau_r)}\right) - 1, \quad (\text{S80}) \\ &= \left(1 + \frac{\tau_c}{\tau_L}\right)^2 \left(1 + \frac{\tau_r}{\tau_L}\right)^2 \left(\frac{(\bar{L}/\sigma_L)^2}{\bar{N}_{\text{eff}}(1-p)^2} + \frac{(\bar{L}/\sigma_L)^2}{p(1-p)\bar{N}_I} \right) \\ &+ \left(1 + \frac{\tau_c}{\tau_L}\right) \left(1 + \frac{\tau_r}{\tau_L}\right) \left(1 + \frac{\tau_c \tau_r}{\tau_L(\tau_c + \tau_r)}\right) - 1, \quad (\text{S81}) \end{aligned}$$

where $\bar{N}_I = f_I \bar{N}_{\text{eff}}$ is the effective number of independent samples, with $f_I = 1/(1+2\tau_c/\Delta)$ the fraction of independent samples (assuming $\tau_r \gg \tau_c$) and $\Delta = 2\tau_r R_T/\bar{N}_{\text{eff}}$ the spacing between the samples. Eq. S81 is indeed the central result of the main text, Eq. 20.

S-V. REWRITING EQ. 20 OF THE MAIN TEXT AS EQ. 23

Modeling the readout system as a sampling device yields an intuitive expression for the sensing error, which shows that the error can be decomposed into a sampling error and a dynamical error (Eq. 20 main text). However, to identify the fundamental resources limiting the sensing accuracy, it is helpful to rewrite the signal-to-noise ratio in terms of collective variables that illuminate the cell resources. For that, we start from Eq. S81 in the previous section (i.e., Eq. 20 of the main text) and we take one step backward in its derivation, by splitting the second term on the right hand side and exploiting the expression for the effective number of independent samples $\bar{N}_I = 1/(1+2\tau_c/\Delta)\bar{N}_{\text{eff}}$ with $\Delta = 2\tau_r R_T/\bar{N}_{\text{eff}}$ (Eq. S80). We then sum up the first two terms on the

right hand side and use that $\bar{N}_{\text{eff}} = q\bar{N} = q\dot{n}\tau_r/p$:

$$\begin{aligned}
\text{SNR}^{-1} &= \left(1 + \frac{\tau_c}{\tau_L}\right)^2 \left(1 + \frac{\tau_r}{\tau_L}\right)^2 \left[\frac{(\bar{L}/\sigma_L)^2}{\bar{N}_{\text{eff}}p(1-p)^2} + \frac{(\bar{L}/\sigma_L)^2}{p(1-p)R_T(1+\tau_r/\tau_c)} \right] \\
&+ \left(1 + \frac{\tau_c}{\tau_L}\right) \left(1 + \frac{\tau_r}{\tau_L}\right) \left(1 + \frac{\tau_c\tau_r}{\tau_L(\tau_c + \tau_r)}\right) - 1 \quad (\text{S82}) \\
&= \left(1 + \frac{\tau_c}{\tau_L}\right)^2 \left(1 + \frac{\tau_r}{\tau_L}\right)^2 \left[\frac{(\bar{L}/\sigma_L)^2}{(1-p)^2q\dot{n}\tau_r} + \frac{(\bar{L}/\sigma_L)^2}{p(1-p)R_T(1+\tau_r/\tau_c)} \right] \\
&+ \left(1 + \frac{\tau_c}{\tau_L}\right) \left(1 + \frac{\tau_r}{\tau_L}\right) \left(1 + \frac{\tau_c\tau_r}{\tau_L(\tau_c + \tau_r)}\right) - 1. \quad (\text{S83})
\end{aligned}$$

This is Eq. 23 of the main text.

S-VI. THE OPTIMAL INTEGRATION TIME

To understand the optimal integration time that maximizes the mutual information, we first write the inverse

signal-to-noise ratio (Eq. S81 or Eq. 20 main text) as

$$\begin{aligned}
\text{SNR}^{-1} &= \underbrace{\frac{1}{\tilde{g}_{L \rightarrow p_{\tau_r}}^2 \sigma_L^2} \left[\frac{p}{\bar{N}_{\text{eff}}} + \frac{p(1-p)}{R_T(1+\tau_r/\tau_c)} \right]}_{\text{sampling error}} \\
&\underbrace{\left(1 + \frac{\tau_c}{\tau_L}\right) \left(1 + \frac{\tau_r}{\tau_L}\right) \left(1 + \frac{\tau_c\tau_r}{\tau_L(\tau_c + \tau_r)}\right)}_{\text{dynamical error}} - 1, \quad (\text{S84})
\end{aligned}$$

where the dynamical gain is given by Eq. S38, namely $\tilde{g}_{L \rightarrow p_{\tau_r}} = p(1-p)/\bar{L}/(1+\tau_c/\tau_L)/(1+\tau_r/\tau_L)$. The first term in between the square brackets is the error in the estimate of p_{τ_r} that comes from the combined effect of the stochasticity in the number of samples, p^2/\bar{N}_{eff} (see Eq. S48), and that which comes from the instantaneous sampling, $p(1-p)/\bar{N}_{\text{eff}}$ (see Eq. S50), while the second term describes the error coming from the correlations between the samples (see Eq. S57). Clearly, decreasing the integration time τ_r helps to reduce the sensing error by increasing the dynamical gain $\tilde{g}_{L \rightarrow p_{\tau_r}}$: this reduces the propagation of the error in the estimate of the receptor occupancy to that in the concentration. Moreover, decreasing τ_r also helps to reduce the dynamical error. On the other hand, decreasing τ_r also compromises the mechanism of time integration by reducing the number of independent measurements per receptor, $(1+\tau_r/\tau_c)$. The interplay between these three effects gives rise to an optimal integration time that maximizes the mutual information.

S-VII. THE OPTIMAL DESIGN

Fig. S1 shows the mutual information $I(L; x^*)$ as a function of the number of receptors R_T and the number of readout molecules X_T for the optimal design of the system, obeying the resource allocation principle of Eq. 31 of the main text. The mutual information is computed via Eq. 23 of the main text, where we have used that $\dot{n}\tau_r = qf(1-f)X_T = qX_T/4$ because $f \rightarrow 1/2$ in the optimal system. Here, τ_r and q are both specified via the optimal allocation principle, Eq. 31 of the main text: for a given X_T and R_T (and τ_c which is kept fixed), the optimal integration time τ_r^* is specified via $X_T = R_T(1+\tau_r^*/\tau_c)$ while $X_T = \beta\dot{w}\tau_r^*$ (Eq. 31) specifies q via $q(\Delta\mu) = (e^{\beta\Delta\mu/2} - 1)^2/(e^{\beta\Delta\mu} - 1) = 4k_B T/\Delta\mu$; solving this for $\Delta\mu$, yields the optimal $\Delta\mu$, $\Delta\mu^{\text{opt}}$, and optimal q , $q^{\text{opt}} \equiv q(\Delta\mu^{\text{opt}})$. With these constraints we can rewrite Eq. 23 of the main text as:

$$\text{SNR}^{-1} = \underbrace{\left(1 + \frac{\tau_c}{\tau_L}\right)^2 \left(1 + \frac{\tau_r^*}{\tau_L}\right)^2}_{\text{dynamical error}} \left[\underbrace{\frac{(\bar{L}/\sigma_L)^2}{p(1-p)R_T(1+\tau_r^*/\tau_c)}}_{\text{receptor input noise}} + \underbrace{\frac{(\bar{L}/\sigma_L)^2}{(1-p)^2 q^{\text{opt},2} X_T/4}}_{\text{coding noise}} \right] - 1, \quad (\text{S85})$$

where τ_r^* is thus specified via $X_T = R_T(1 + \tau_r^*/\tau_c)$.

Fig. S1 shows the mutual information $I(L; x^*)$ computed via Eq. S85 as a function of R_T and X_T , with τ_r^* specified via $X_T = R_T(1 + \tau_r^*/\tau_c)$. It is seen that for a given X_T the mutual information is maximized for $R_T = X_T$. This corresponds to $\tau_r^* = 0$: the system has become an instantaneous responder and has given up on time integration. In this limit the power diverges. In fact, an equilibrium sensing precision would be superior, because it can reach the same precision but does not need to burn fuel [13]. The observation that the membrane is highly packed suggests that sensing systems employ time integration because R_T is limiting. This leads to the design principle of Eq. 32 of the main text, $R_T(1 + \tau_r^{\text{opt}}/\tau_c) = X_T^{\text{opt}} = \beta \dot{w}^{\text{opt}} \tau_r^{\text{opt}}$, where τ_r^{opt} is computed in the R_T -limiting regime (i.e. via Eq. 24 main text). This design principle maximizes the sensing precision for a given R_T , and minimizes the number of readout molecules X_T and the power \dot{w} needed to reach that precision.

APPENDIX S-A: THE VARIANCES AND CO-VARIANCES

In the Fourier space we obtain as solutions of Eqs. S6 and S7

$$\delta \tilde{R}L(\omega) = \frac{\tilde{\eta}_{RL}}{\mu + i\omega} + \frac{\rho \delta \tilde{L}(\omega)}{\mu + i\omega} \quad (\text{S86})$$

$$\delta x^*(\omega) = \frac{\tilde{\eta}_{x^*}}{\mu' + i\omega} + \frac{\rho' \delta \tilde{R}L(\omega)}{\mu' + i\omega}. \quad (\text{S87})$$

The corresponding power spectra $S_y(\omega) = (1/2T)\langle \delta \tilde{y}(\omega) \delta \tilde{y}(-\omega) \rangle$ of $y = L, RL, x^*$ are then given by the spectral addition rule [51, 52]

$$S_L(\omega) = \frac{2\lambda \sigma_L^2}{\lambda^2 + \omega^2} \quad (\text{S88})$$

$$S_{RL}(\omega) = \frac{\langle \eta_{RL}^2 \rangle}{\mu^2 + \omega^2} + \frac{\rho^2 S_{\delta L}(\omega)}{\mu^2 + \omega^2} \quad (\text{S89})$$

$$S_{x^*}(\omega) = \frac{\langle \eta_{x^*}^2 \rangle}{\mu'^2 + \omega^2} + \frac{\rho'^2 S_{\delta RL}(\omega)}{\mu'^2 + \omega^2}, \quad (\text{S90})$$

while the cross power spectra $S_{yz}(\omega) = 1/(2T)\langle \delta \tilde{y}(\omega) \delta \tilde{z}(-\omega) \rangle$ are

$$S_{L,RL}(\omega) = \frac{2k\rho}{(\lambda^2 + \omega^2)(\mu - i\omega)} \quad (\text{S91})$$

$$S_{L,x^*}(\omega) = \frac{2k\rho\rho'}{(\lambda^2 + \omega^2)(\mu - i\omega)(\mu' - i\omega)} \quad (\text{S92})$$

$$S_{RL,x^*}(\omega) = \frac{\rho' \langle \eta_{RL}^2 \rangle}{(\mu^2 + \omega^2)(\mu' - i\omega)} + \frac{2k\rho^2\rho'}{(\mu^2 + \omega^2)(\lambda^2 + \omega^2)(\mu' - i\omega)}. \quad (\text{S93})$$

We can now compute the noise strengths by integration, $\sigma_{yz}^2 = 1/(2\pi) \int_{-\infty}^{\infty} d\omega S_{yz}(\omega)$, resulting in the correlation matrix

$$\Sigma = \begin{pmatrix} \sigma_L^2 & \sigma_{L,RL}^2 & \sigma_{L,x^*}^2 \\ \sigma_{L,RL}^2 & \sigma_{RL}^2 & \sigma_{RL,x^*}^2 \\ \sigma_{L,x^*}^2 & \sigma_{RL,x^*}^2 & \sigma_{x^*}^2 \end{pmatrix}$$

with matrix elements

$$\sigma_{x^*}^2 = f(1-f)X_T + \frac{\rho'^2}{\mu'(\mu + \mu')} \left[p(1-p)R_T + \frac{\rho^2 \sigma_L^2 (\lambda + \mu + \mu')}{\mu(\lambda + \mu)(\lambda + \mu')} \right], \quad (\text{S94})$$

$$\sigma_{RL}^2 = p(1-p)R_T + \frac{\rho^2 \sigma_L^2}{\mu(\mu + \lambda)}, \quad (\text{S95})$$

$$\sigma_{L,RL}^2 = \frac{\rho \sigma_L^2}{(\mu + \lambda)}, \quad (\text{S96})$$

$$\sigma_{L,x^*}^2 = \frac{\rho \rho' \sigma_L^2}{(\lambda + \mu)(\lambda + \mu')}, \quad (\text{S97})$$

$$\sigma_{RL,x^*}^2 = \frac{\rho'}{\mu' + \mu} \left[p(1-p)R_T + \frac{\rho^2 \sigma_L^2 (\mu' + \lambda + \mu)}{\mu(\lambda + \mu)(\lambda + \mu')} \right]. \quad (\text{S98})$$

APPENDIX S-B: VARIANCE IN AVERAGE RECEPTOR OCCUPANCY FOR FIXED NUMBER OF SAMPLES

Eq. S50 gives the variance in the average receptor occupancy for a fixed number of samples. To derive it, we note that

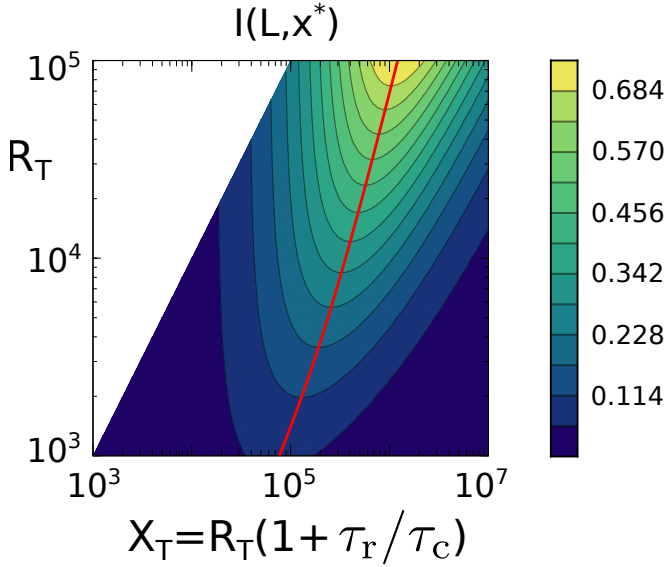


FIG. S1. The mutual information $I(L; x^*)$ computed via Eq. S85 as a function of R_T and X_T for the optimal system that obeys the optimal resource allocation principle Eq. 31 of the main text: $R_T(1 + \tau_r^*/\tau_c) = X_T = \beta \dot{w}_r^*$. It is seen that for a given X_T , the mutual information is maximized for $R_T = X_T$. This corresponds to $\tau_r^* = 0$, which minimizes the dynamical error: the system has given up on time integration. However, in this limit, the power diverges. In fact, an equilibrium sensing system would be superior, because it can reach, for the same number of receptors, the same sensing precision as a non-equilibrium one that does not time integrate, without turning over costly fuel [13]. The observation that the membrane is very crowded suggests that the number of receptors is limiting. This leads to the design principle of Eq. 32 of the main text: $R_T(1 + \tau_r^{\text{opt}}/\tau_c) = X_T^{\text{opt}} = \beta \dot{w}_r^{\text{opt}}$; here, the optimal integration time τ_r^{opt} is computed for a given R_T assuming R_T is limiting (Eq. 24 main text), while the optimal number of readout molecules X_T^{opt} and the optimal power \dot{w}_r^{opt} are then set by this equation. This optimizes the design of the network for a given number of receptors R_T : X_T^{opt} and \dot{w}_r^{opt} are adjusted to R_T such that they are neither in excess nor limiting. Indeed, the contour plot above shows that for a given R_T there is an optimal X_T , indicated by the red line; this value of X_T is close to that given by $X_T^{\text{opt}} = R_T(1 + \tau_r^{\text{opt}}/\tau_c)$ because τ_r^{opt} , which is computed assuming X_T is in excess ($X_T \rightarrow \infty$), is close to the optimal τ_r that is computed assuming $X_T \approx R_T(1 + \tau_r/\tau_c)$ (the resources limit sensing like weak links in a chain, see also Fig. 3(a)). Parameters: $\tau_c/\tau_L = 10^{-2}$; $\sigma_L/\bar{L}_T = 10^{-2}$; p optimized; q^{opt} given by $q(\Delta\mu) = 4k_B T/\Delta\mu$ such that $X_T = \beta \dot{w}_r^*$.

$$\text{var} \left(\frac{\sum_{i=1}^N n_i(t_i)}{N} \middle| N \right)_{\delta L(t)} \quad (\text{S99})$$

$$= \frac{E \langle (\sum_{i=1}^N n_i(t_i))^2 \rangle_{\delta L(t)} - E \langle \sum_{i=1}^N n_i(t_i) \rangle_{\delta L(t)}^2}{N^2} \quad (\text{S100})$$

$$= \frac{E \langle (\sum_{i=1}^N n_i(t_i))^2 \rangle_{\delta L(t)} - N^2 (p + \tilde{g} \delta L(t))^2}{N^2} \quad (\text{S101})$$

$$= \frac{N(p + \tilde{g} \delta L(t)) + N(N-1) \overline{E \langle n_i(t_i) n_j(t_j) \rangle_{\delta L(t)}}}{N^2} - \frac{(p + \tilde{g} \delta L(t))^2}{N^2} \quad (\text{S102})$$

$$= \frac{N(p + \tilde{g} \delta L(t)) - N(p + \tilde{g} \delta L(t))^2}{N^2} + \frac{N(N-1) \overline{E \langle \tilde{\delta} n_i(t_i) \tilde{\delta} n_j(t_j) \rangle_{\delta L(t)}}}{N^2} \quad (\text{S103})$$

$$= \frac{p(1-p) - \tilde{g}^2 \sigma_L^2}{N} + \frac{N(N-1) \overline{E \langle \tilde{\delta} n_i(t_i) \tilde{\delta} n_j(t_j) \rangle_{\delta L(t)}}}{N^2} \quad (\text{S104})$$

Here $\tilde{\delta} n_i(t_i) \equiv n_i(t_i) - (p + \langle n_i(t_i) \rangle_{\delta L(t)})$ is the deviation away from the average receptor occupancy $p + \langle n_i(t_i) \rangle_{\delta L(t)}$ when the ligand concentration at time t is $\delta L(t)$. Here, E denotes an average over the sampling times of the receptor. The average of $n_i(t_i)$ over the sampling times t_i given $\delta L(t)$, is $E[\langle n_i(t_i) \rangle_{\delta L(t)}] = p + \tilde{g} \delta L(t)$ (see Eqs. S34 and S37). In addition, $\sigma_L^2 = \langle \delta L(t)^2 \rangle$ is the variance of the ligand concentration, and in going from Eq. S101 to Eq. S102 we have exploited that $n^2 = n$. The quantity $\overline{E \langle \tilde{\delta} n_i(t_i) \tilde{\delta} n_j(t_j) \rangle_{\delta L(t)}}$ is the co-variance of the receptor occupancy given that the ligand concentration at time t is $\delta L(t)$, and then averaged over all values of $\delta L(t)$, as indicated by the overline. This quantity has a contribution from the receptor switching noise and the dynamical error resulting from the ligand fluctuations.

While $\overline{E \langle \tilde{\delta} n_i(t_i) \tilde{\delta} n_j(t_j) \rangle_{\delta L(t)}} = \overline{E \langle n_i(t) n_j(t) \rangle_{\delta L(t)}} - \overline{E \langle n_i \rangle_{\delta L(t)} \langle n_j \rangle_{\delta L(t)}}$ is the quantity that we need to compute, it is difficult to compute straightforwardly. We can however exploit the following trick [30]. Denoting $x = n_i(t_i)$, $y = n_j(t_j)$ and $z = \delta L(t)$, we can write the quantity of interest as $\overline{E \langle \tilde{\delta} n_i(t_i) \tilde{\delta} n_j(t_j) \rangle_{\delta L(t)}} = \overline{E \langle xy \rangle_z} - \overline{E \langle x \rangle_z E \langle y \rangle_z}$. We can then exploit the following relation

$$\overline{E \langle \delta x \delta y \rangle_z} = \overline{E \langle xy \rangle_z} - \overline{E \langle x \rangle_z E \langle y \rangle_z} + \overline{E \langle x \rangle_z E \langle y \rangle_z} - \overline{E \langle x \rangle_z} \overline{E \langle y \rangle_z}, \quad (\text{S105})$$

$$= \overline{E \langle xy \rangle_z} - \overline{E \langle x \rangle_z E \langle y \rangle_z} + \tilde{g}^2 \sigma_L^2 \quad (\text{S106})$$

Importantly, $\overline{E \langle \delta x \delta y \rangle_z}$ is the co-variance related to the deviation of the receptor occupancy from the mean p , which is easier to compute than the deviation from $p +$

$\tilde{g}\delta L(t)$. Inserting the above result into Eq. S104 yields

$$\begin{aligned} \text{var} \left(\frac{\sum_{i=1}^N n_i(t_i)}{N} \right)_{\delta L(t)} &= \frac{p(1-p)}{N} + \overline{E\langle \delta n_i(t_i) \delta n_j(t_j) \rangle}_{\delta L(t)} - \tilde{g}^2 \sigma_L^2 \quad (\text{S107}) \end{aligned}$$

where we have used that $N(N-1) \approx N^2$ for $N \gg 1$.

APPENDIX S-C: THE RELIABILITY FACTOR q

Here we derive the expression for the reliability factor q in terms of the fundamental rate constants, k_f , k_{-f} , k_r , k_{-r} , which is used to derive the principal result of the main text, Eq. 20 (i.e. Eq. S81 above). We first note that

$$\begin{aligned} e^{\beta\Delta\mu_1} - 1 &= \frac{k_f \bar{x}}{k_{-f} \bar{x}^*} - 1 \\ &= \frac{k_f(k_r + k_{-f}pR_T)}{k_{-f}(k_{-r} + k_f pR_T)} - 1 = \frac{k_f k_r - k_{-f} k_{-r}}{k_{-f}(k_{-r} + k_f pR_T)}. \quad (\text{S108}) \end{aligned}$$

$$\begin{aligned} e^{\beta\Delta\mu_2} - 1 &= \frac{k_r \bar{x}}{k_{-r} \bar{x}} - 1 \\ &= \frac{k_r(k_{-r} + k_{-f}pR_T)}{k_{-r}(k_r + k_{-f}pR_T)} - 1 = \frac{(k_f k_r - k_{-f} k_{-r})pR_T}{k_{-r}(k_r + k_{-f}pR_T)}. \quad (\text{S109}) \end{aligned}$$

Noting that $\Delta\mu = \Delta\mu_1 + \Delta\mu_2$, we find that

$$e^{\beta\Delta\mu} - 1 = \frac{k_f k_r}{k_{-f} k_{-r}} - 1 = \frac{k_f k_r - k_{-f} k_{-r}}{k_{-f} k_{-r}}. \quad (\text{S110})$$

Combining the above results yields the reliability factor q :

$$\begin{aligned} q &\equiv \frac{(e^{\beta\Delta\mu_1} - 1)(e^{\beta\Delta\mu_2} - 1)}{e^{\beta\Delta\mu} - 1} \\ &= \frac{(k_f k_r - k_{-f} k_{-r})pR_T}{(k_{-r} + k_f pR_T)(k_r + k_{-f} pR_T)} \quad (\text{S111}) \end{aligned}$$

In order to obtain an expression for the reliability factor q that does not explicitly depend on the rate constants, we notice that the flux of readout activation \dot{n} can be expressed as

$$\begin{aligned} \dot{n} &\equiv k_f \overline{RL\bar{x}} - k_{-f} \overline{RLx^*} \\ &= k_f pR_T(1-f)X_T - k_{-f} pR_T f X_T \\ &= pR_T X_T [k_f(1-f) - k_{-f} f] \\ &= pR_T X_T [k_f(k_{-f} pR_T + k_r)\tau_r - k_{-f}(k_f pR_T + k_{-r})\tau_r] \\ &= pR_T X_T \tau_r (k_f k_r - k_{-f} k_{-r}), \quad (\text{S112}) \end{aligned}$$

where in the fourth line we have exploited that $f = (k_f pR_T + k_{-r})\tau_r$. Substituting $(k_f k_r - k_{-f} k_{-r})pR_T = \dot{n}/(X_T \tau_r)$ into Eq. S111 and exploiting again the expression for f yields for the reliability factor q

$$q = \frac{\dot{n}\tau_r}{f(1-f)X_T}. \quad (\text{S113})$$

This expression shows that the flux \dot{n} can also be expressed as a function of q , namely

$$\dot{n} = f(1-f)X_T q / \tau_r. \quad (\text{S114})$$

Finally, the reliability factor q can also be expressed in terms of the variable $\rho' = k_f(1-f)X_T - k_{-f}fX_T$ by rewriting the flux \dot{n} as

$$\dot{n} = pR_T X_T [k_f(1-f) - k_{-f}f] = \rho' pR_T, \quad (\text{S115})$$

yielding for q

$$q = \frac{\rho' pR_T \tau_r}{f(1-f)X_T}. \quad (\text{S116})$$

-
- [1] H.C. Berg and E.M. Purcell. Physics of chemoreception. *Biophys. J.*, 20(2):193–219, November 1977.
- [2] V. Sourjik and H.C. Berg. Receptor sensitivity in bacterial chemotaxis. *Proc. Natl. Acad. Sci. USA*, 99(1):123–127, 2002.
- [3] M. Ueda and T. Shibata. Stochastic signal processing and transduction in chemotactic response of eukaryotic cells. *Biophys. J.*, 93(1):11–20, 2007.
- [4] W. Bialek and S. Setayeshgar. Physical limits to biochemical signaling. *Proc. Natl. Acad. Sci. USA*, 102(29):10040–10045, 2005.
- [5] K. Wang, W.J. Rappel, R. Kerr, and H. Levine. Quantifying noise levels of intercellular signals. *Phys. Rev. E*, 75(6):061905, 2007.
- [6] W.J. Rappel and H. Levine. Receptor noise and directional sensing in eukaryotic chemotaxis. *Phys. Rev. Lett.*, 100(22):228101, 2008.
- [7] R.G. Endres and N.S. Wingreen. Maximum likelihood and the single receptor. *Phys. Rev. Lett.*, 103(15):158101, 2009.
- [8] B. Hu, W. Chen, W.J. Rappel, and H. Levine. Physical limits on cellular sensing of spatial gradients. *Phys. Rev. Lett.*, 105(4):048104, 2010.
- [9] T. Mora and N.S. Wingreen. Limits of sensing temporal concentration changes by single cells. *Phys. Rev. Lett.*, 104(24):248101, 2010.

- [10] P. Mehta and D.J. Schwab. Energetic Costs of Cellular Computation. *Proc. Natl. Acad. Sci. USA*, 109(44):17978, 2012.
- [11] C.C. Govern and P.R. ten Wolde. Fundamental limits on sensing chemical concentrations with linear biochemical networks. *Phys. Rev. Lett.*, 109:218103, 2012.
- [12] C.C. Govern and P.R. ten Wolde. Optimal resource allocation in cellular sensing systems. *Proc. Natl. Acad. Sci. USA*, 111(49):17486–17491, 2014.
- [13] C.C. Govern and P.R. ten Wolde. Energy Dissipation and Noise Correlations in Biochemical Sensing. *Phys. Rev. Lett.*, 113:258102, 2014.
- [14] K. Kaizu, W. De Ronde, J. Paijmans, K. Takahashi, F. Tostevin, and P.R. ten Wolde. The Berg-Purcell limit revisited. *Biophysical Journal*, 106(4):976–985, 2014.
- [15] A. Mugler, A. Levchenko, and I. Nemenman. Limits to the precision of gradient sensing with spatial communication and temporal integration. *Proc. Natl. Acad. Sci. USA*, 113(6):E689–E695, February 2016.
- [16] S. Fancher and A. Mugler. Fundamental limits to collective concentration sensing in cell populations. *Phys. Rev. Lett.*, 118(7):078101, February 2017.
- [17] P.R. ten Wolde, N.B. Becker, T.E. Ouldridge, and A. Mugler. Fundamental limits to cellular sensing. *J. Stat. Phys.*, 162(5):1395–1424, January 2016.
- [18] N.B. Becker, A. Mugler, and P.R. ten Wolde. Optimal prediction by cellular signaling networks. *Phys. Rev. Lett.*, 115:258103, 2015.
- [19] L. Durrieu, D. Kirrmaier, T. Schneidt, I. Kats, S. Raghavan, L. Hufnagel, T.E. Saunders, and M. Knop. Bicoid gradient formation mechanism and dynamics revealed by protein lifetime analysis. *Mol. Syst. Biol.*, 14(9):e8355–15, 2018.
- [20] F. Tostevin and P.R. ten Wolde. Mutual information between input and output trajectories of biochemical networks. *Phys. Rev. Lett.*, 102:218101, 2009.
- [21] P. Sartori and Y. Tu. Noise filtering strategies in adaptive biochemical signaling networks. *J. Stat. Phys.*, 142(6):1206–1217, 2011.
- [22] J. Long, S.W. Zucker, and T. Emonet. Feedback between motion and sensation provides nonlinear boost in run-and-tumble navigation. *PLoS Comput. Biol.*, 13(3):e1005429, 2017.
- [23] M. Monti, D.K. Lubensky, and P.R. ten Wolde. Robustness of clocks to input noise. *Phys. Rev. Lett.*, 121(7):078101, 2018.
- [24] A Goldbeter and D E Koshland. An amplified sensitivity arising from covalent modification in biological systems. *Proc. Natl. Acad. Sci. U. S. A.*, 78(11):6840–6844, 1981.
- [25] U. Alon. *Introduction to Systems Biology: Design Principles of Biological Networks*. CRC press, Boca Raton, FL, 2007.
- [26] A.H. Lang, C.K. Fisher, T. Mora, and P. Mehta. Thermodynamics of statistical inference by cells. *Phys. Rev. Lett.*, 113(14):148103, 2014.
- [27] D. Hartich and U. Seifert. Optimal inference strategies and their implications for the linear noise approximation. *Phys. Rev. E*, 94(4):042416–11, 2016.
- [28] F. Tostevin and P.R. ten Wolde. Mutual information in time-varying biochemical systems. *Phys. Rev. E*, 81:061917, 2010.
- [29] A. Hilfinger and J. Paulsson. Separating intrinsic from extrinsic fluctuations in dynamic biological systems. *Proc. Natl. Acad. Sci. USA*, 108(29):12167–12172, 2011.
- [30] C.G. Bowsher, M. Voliotis, and P.S. Swain. The fidelity of dynamic signaling by noisy biomolecular networks. *PLoS Comput. Biol.*, 9(3), 2013.
- [31] Because the system is stationary and time-invariant, we can omit the argument in $L(t)$ and write $L = L(t)$.
- [32] T.E. Ouldridge, C.C. Govern, and P.R. ten Wolde. Thermodynamics of computational copying in biochemical systems. *Phys. Rev. X*, 7(2):021004, 2017.
- [33] M. Li and G.L. Hazelbauer. Cellular stoichiometry of the components of the chemotaxis signaling complex. *J. Bacteriol.*, 186(12):3687–3694, 2004.
- [34] A. Vaknin and H.C. Berg. Physical responses of bacterial chemoreceptors. *J. Mol. Biol.*, 366(5):1416–1423, 2007.
- [35] M.A. Danielson, H.P. Biemann, D.E. Koshland, Jr. Falke, and J.J. Falke. Attractant- and disulfide-induced conformational changes in the ligand binding domain of the chemotaxis aspartate receptor: a 19F NMR study. *Biochemistry*, 33(20):6100–6109, 1994.
- [36] H.C. Berg and D.A. Brown. Chemotaxis in *Escherichia coli* analysed by three-dimensional tracking. *Nature*, 239(5374):500–504, 1972.
- [37] K.M. Taute, S. Gude, S.J. Tans, and T.S. Shimizu. High-throughput 3D tracking of bacteria on a standard phase contrast microscope. *Nat. Commun.*, 6:1–9, 2015.
- [38] L. Jiang, Q. Ouyang, and Y. Tu. Quantitative modeling of *Escherichia coli* chemotactic motion in environments varying in space and time. *PLoS Comput. Biol.*, 6(4):e1000735–12, 2010.
- [39] M. Flores, T.S. Shimizu, P.R. ten Wolde, and F. Tostevin. Signaling noise enhances chemotactic drift of *E. coli*. *Phys. Rev. Lett.*, 109(14):148101, 2012.
- [40] T.S. Shimizu, Y. Tu, and H.C. Berg. A modular gradient-sensing network for chemotaxis in *Escherichia coli* revealed by responses to time-varying stimuli. *Mol. Syst. Biol.*, 6:1–14, 2010.
- [41] V. Sourjik and H.C. Berg. Binding of the *Escherichia coli* response regulator CheY to its target measured in vivo by fluorescence resonance energy transfer. *Proc. Natl. Acad. Sci. USA*, 99(20):12669–12674, 2002.
- [42] Monica Skoge, Yigal Meir, and Ned S Wingreen. Dynamics of cooperativity in chemical sensing among cell-surface receptors. *Phys. Rev. Lett.*, 107:178101, 2011.
- [43] A.C. Barato, D. Hartich, and U. Seifert. Efficiency of cellular information processing. *New J. Phys.*, 16:103024, 2014.
- [44] J.M. Horowitz and M. Esposito. Thermodynamics with continuous information flow. *Phys. Rev. X*, 4:031015, 2014.
- [45] D. Hartich, A.C. Barato, and U. Seifert. Sensory capacity: An information theoretical measure of the performance of a sensor. *Phys. Rev. E*, 93(2):022116–14, 2016.
- [46] R.A. Brittain, N.S. Jones, and T.E. Ouldridge. What we learn from the learning rate. *J. Stat. Mech.*, 2017(6):063502–22, 2017.
- [47] G. Lan, P. Sartori, S. Neumann, V. Sourjik, and Y. Tu. The energy–speed–accuracy trade-off in sensory adaptation. *Nat. Phys.*, 8(5):422–428, 2012.
- [48] P. Sartori and Y. Tu. Free energy cost of reducing noise while maintaining a high sensitivity. *Phys. Rev. Lett.*, 115(11):118102, 2015.
- [49] D.T. Gillespie. The chemical Langevin equation. *J. Chem. Phys.*, 113(1):297–306, 2000.
- [50] C.W. Gardiner. *Stochastic methods*. Springer-Verlag, Berlin–Heidelberg–New York–Tokyo, 2009.

- [51] P.B. Warren, S. Tănase-Nicola, and P.R. ten Wolde. Exact results for noise power spectra in linear biochemical reaction networks. *J. Chem. Phys.*, 125(14):144904, 2006.
- [52] S. Tanase-Nicola, P.B. Warren, and P.R. ten Wolde. Signal detection, modularity, and the correlation between extrinsic and intrinsic noise in biochemical networks. *Phys. Rev. Lett.*, 97:068102, 2006.
- [53] A.M. Walczak, A. Mugler, and C.H. Wiggins. Analytic methods for modeling stochastic regulatory networks. *Computational Modeling of Signaling Networks*, 880:273–322, 2012.
- [54] N. G. Van Kampen. *Stochastic processes in physics and chemistry*. North Holland, Amsterdam, 1992.
- [55] E. Ziv, I. Nemenman, and C.H. Wiggins. Optimal signal processing in small stochastic biochemical networks. *PLoS ONE*, 2(10):e1077, 2007.
- [56] C. Shannon. *Bell Syst. Tech. J.*, 27:623, 1948.
- [57] S.G. Das, M. Rao, and G. Iyengar. Universal lower bound on the free-energy cost of molecular measurements. *Phys. Rev. E*, 95(6):062410, 2017.